



1 **Insights on the water mean transit time in a high-elevation**
2 **tropical ecosystem**

3

4 **G. M. Mosquera^{1,2}, C. Segura³, K. B. Vaché², D. Windhorst⁴, L. Breuer^{4,5} and**
5 **Patricio Crespo¹**

6 [1]{Departamento de Recursos Hídricos y Ciencias Ambientales & Facultad de Ciencias
7 Agropecuarias, Universidad de Cuenca, Av. 12 de Abril, Cuenca, Ecuador }

8 [2]{Department of Biological and Ecological Engineering, Oregon State University,
9 Corvallis, OR, USA }

10 [3]{Department of Forestry Engineering, Resources, and Management, Oregon State
11 University, Corvallis, Oregon, USA }

12 [4]{Institute for Landscape Ecology and Resources Management (ILR), Research Centre for
13 BioSystems, Land Use and Nutrition (IFZ), Justus Liebig University Gießen, Gießen,
14 Germany }

15 [5]{Centre for International Development and Environmental Research, Justus Liebig
16 University Gießen, Gießen, Germany }

17 Correspondence to: G. M. Mosquera. (giovanny.mosquerar@ucuenca.edu.ec)

18

19 **Abstract**

20 This study focuses on the investigation of the yet unknown mean transit time (MTT) of
21 stream waters and its spatial variability in tropical alpine ecosystems (wet Andean páramo).
22 The study site is the Zhurucay River Ecohydrological Observatory (7.53 km²) located in south
23 Ecuador. A lumped parameter model considering five transit time distribution (TTD)
24 functions was used to estimate MTTs. We used a unique data set of $\delta^{18}\text{O}$ and $\delta^2\text{H}$ isotopic
25 composition of rainfall and streamflow water samples collected for three years (May 2011-
26 May 2014) in a nested monitoring system of streams. Linear regression between MTT and



1 landscape (soil and vegetation cover, geology, and topography) and hydrometric (runoff
2 coefficient and specific discharge rates) variables was used to determine controls on MTT
3 variability, as well as mean electrical conductivity (MEC) as a possible proxy for MTT.
4 Results revealed that the exponential TTD function best describes the hydrology of the site,
5 indicating a relatively simple transition from rainfall water to the streams through the organic
6 horizon of the wet páramo soils. MTT of the streams is relatively short (0.15-0.73 yr, 53-264
7 days). Regression analysis revealed negative correlation between the catchment's average
8 slope and MTT ($R^2 = 0.78$, $p < 0.05$). MTT showed no significant correlation with
9 hydrometric variables whereas MEC increases with MTT ($R^2 = 0.89$ $p < 0.001$). Overall, we
10 conclude that: 1) MTT of streams confirms that the hydrology of the ecosystem is dominated
11 by shallow subsurface flow; 2) the interplay between the high storage capacity of the wet
12 páramo soils and the slope of the catchments provides the ecosystem with high regulation
13 capacity; and 3) MEC is an efficient predictor of MTT variability in this system of catchments
14 with relatively homogeneous geology.

15 Keywords: Ecohydrological processes, subsurface flow, mean transit time, lumped parameter
16 model, Andosol and Histosol, wet Andean páramo, tropical wetlands, South America

17

18 **1 Introduction**

19 Investigating ecohydrological processes by identifying fundamental catchment descriptors –
20 such as the MTT of waters – i.e., the average time elapsed since a water molecule enters a
21 catchment as recharge to when it exits it at some discharge point (Bethke and Johnson, 2002;
22 Etcheverry and Perrochet, 2000; Rodhe et al., 1996) – is fundamental in order to: 1) advance
23 global hydrological, ecological, and geochemical processes understanding and 2) improve the
24 management of water resources. This is particularly critical in high-elevation tropical
25 environments, such as the wet Andean páramo (further referred as “páramo”), in which,
26 hydrological knowledge remains limited, despite its importance as the major water provider
27 for more than 100 million people in the region (IUCN, 2002). Water originated from the
28 páramo sustains the socio-economic development in this region by fulfilling urban,
29 agricultural, industrial, and hydropower generation water needs (Célleri and Feyen, 2009).



1 Despite the importance of tropical biomes as natural sources and regulators of streamflow,
2 there are very few studies of MTT in tropical environments (e.g., Roa-García and Weiler,
3 2010; Timbe et al., 2014). The majority of MTT studies have been conducted in catchments
4 with strong climate seasonality, i.e., located in the northern and southern hemispheres (e.g.,
5 McGlynn and McDonnell, 2003; McGuire and McDonnell, 2006; McGuire et al., 2005), and
6 considerably less attention has been devoted to tropical environments. Most tracer-based
7 studies conducted in tropical latitudes focused on isotope hydrograph separation at storm
8 event scale (e.g., Goller et al., 2005; Muñoz-Villers and McDonnell, 2012), the isotopic
9 characterization of precipitation patterns (e.g., Vimeux et al., 2011; Windhorst et al., 2013),
10 and the identification of ecohydrological processes (e.g., Crespo et al., 2012; Goldsmith et al.,
11 2012; Mosquera et al., In review). However, studies focusing on MTTs in order to improve
12 the understanding of rainfall-runoff processes and their dependence on landscape biophysical
13 features in tropical regions are still lacking and urgently needed in order to improve water
14 resources management.

15 Prior investigations in our study site suggest that runoff originates from the shallow organic
16 horizon of the páramo soils located near the streams (Histosol soils or Andean wetlands), thus
17 favoring shallow subsurface flow; whereas deep groundwater contributions to discharge are
18 minimal (Mosquera et al., 2015, In review). The hydrological importance of shallow
19 subsurface flow to runoff generation has also been demonstrated in a variety of ecosystems
20 around the globe (e.g., Freeze, 1972; Hewlett, 1961; Penna et al., 2011), but yet, the MTT of
21 stream waters in these systems has not been explored in tropical regions. Therefore, our study
22 site provides a unique opportunity to gain understanding of the MTT of a shallow subsurface
23 flow dominated system in a tropical setting. In addition, the study of the MTT in natural
24 wetland systems has been limited to sites located in northern boreal catchments in Sweden
25 (Lyon et al., 2010), and peatlands, which are hydrogeologically comparable to the Histosols
26 soils in our study site, in Scottish mountainous regions (e.g., Hrachowitz et al., 2009a;
27 Tetzlaff et al., 2014). Nevertheless, given that these catchments have significant contributions
28 from spring snowmelt and groundwater contributions to discharge, respectively, neither of
29 these allows for the isolation of the effect of wetlands in the subsurface transport of the water
30 within the catchments.



1 Another critical issue is the identification of controls on the MTT of stream waters. As
2 detailed observations of combined hydrometric and isotopic information are not feasible in
3 many regions due to limited funding and site accessibility, identifying controls of MTT
4 variability in nested and paired monitoring systems of streams is fundamental towards
5 regionalization of ecohydrological processes (Hrachowitz et al., 2009a) and prediction in
6 ungauged basins (Tetzlaff et al., 2010). Yet, investigation of controls on MTT variability is
7 still fairly scarce (Tetzlaff et al., 2013). Most studies have found that MTT scales with
8 topographic and/or hydrogeological controls. For instance, topographical controls on MTT
9 variability were found in New Zealand catchments (Broxton et al., 2009) and a system of
10 streams in Oregon, USA (McGuire et al., 2005); whereas the proportion of wetlands and
11 responsive soils were reported as major MTT controls in Swedish catchments (Lyon et al.,
12 2010) and Scottish streams (Soulsby et al., 2006), respectively.

13 In this study, we seek to add to the current geographical scope of MTT studies by addressing
14 two questions which remain open in hydrological science and have received little attention in
15 high-elevation tropical ecosystems: “How old is stream water?” (McDonnell et al., 2010) and
16 “How does landscape structure influence catchment transit time across different geomorphic
17 provinces?” (Tetzlaff et al., 2009). Detailed hydrometric observations that highlighted
18 subsurface dominated rainfall-runoff response (Crespo et al., 2011; Mosquera et al., In
19 review) together with information of the landscape biophysical characteristics in our páramo
20 study site will allow for process-based understanding regarding: i) the spatial variability of
21 MTT and ii) the factors controlling such variability. Based on our current knowledge of the
22 hydrology of the ecosystem, i.e., apparent dominance of shallow subsurface flow to runoff
23 generation, we hypothesize relatively short MTTs of streams compared to systems dominated
24 by groundwater contributions to discharge. Also, based on the hydrogeological and climatic
25 similarities between our páramo site and the peatland-podzols dominated ecosystems in the
26 Scottish highlands (e.g., Soulsby et al., 2006; Tetzlaff et al., 2014), we hypothesize the
27 proportion of wetlands to be a dominant control on the variability of the MTT in this high-
28 elevation tropical ecosystem.



1 **2 Materials and methods**

2 **2.1 Study site**

3 The Zhuruca River Ecohydrological Observatory is a basin located within a tropical alpine
4 biome, locally known as wet Andean páramo. It is situated in south Ecuador (3°04'S,
5 79°14'W) on the west slope of the Atlantic-Pacific continental divide and discharges into the
6 Jubones River (Pacific Ocean tributary). The basin has a drainage area of 7.53 km² and
7 extends within an elevation range of 3400 to 3900 m a.s.l. Climate is controlled by the Pacific
8 regime, although it is also influenced by the Amazonian regime to a lesser extent. Mean
9 annual precipitation at the observatory is 1345 mm at 3780 m a.s.l. Precipitation shows low
10 seasonality with two relatively drier months (August and September) and primarily falls as
11 drizzle (Padrón et al., 2015). Mean annual temperature is 6.0 °C at 3780 m a.s.l. and 9.2 °C at
12 3320 m a.s.l. (Córdova et al., 2015).

13 Geology primarily corresponds to volcanic rock deposits compacted by glacial activity during
14 the last ice age (Coltorti and Ollier, 2000). The Quimsacocha formation covers the northern
15 part of the basin and its lithology is composed by basaltic flows with plagioclases, feldspars,
16 and andesitic pyroclastics. The Turi formation covers the southern part of the catchment and
17 its lithology mainly corresponds to tuffaceous andesitic breccias, conglomerates, and
18 horizontally stratified sands. Both formations date from the late Miocene period (Pratt et al.,
19 1997). The geomorphology of the landscape bears the imprint of glaciated U-shaped valleys.
20 The average slope of the basin is 17%. The majority of the basin (72%) has mean gradients
21 between 0%-20%, although slopes up to 40% are also found (24%). There is an interesting
22 geomorphic feature in the northeastern side of the basin corresponding to a ponded wetland at
23 a flat hilltop. As indicated by geologists from INV metals mining company, this structure
24 most likely resulted from the eutrophication of a lagoon due to high accumulation of volcanic
25 material. This area is locally known as “Laguna Ciega” (“Blind Lagoon” in Spanish) and
26 drains towards the outlet of catchment M7 (see Figure 1). The analysis of the water stable
27 isotopic composition of soil water and streamflow in this area indicated that the hydrologic
28 processes of this site occur in the shallow ponded water that is directly connected to the



1 drainage network; while deeper water stored in the soil profile has little influence for
2 discharge generation most likely as a results of the eutrophic condition of the wetland
3 (Mosquera et al., In review).

4 Andosols, mainly found in the hillslopes, are the dominant soil type in the study site, covering
5 approximately 80% of the total basin area. Histosols (Andean wetlands), mainly found in flat
6 areas where rock geomorphology allows water accumulation cover the remaining portion of
7 the basin (Mosquera et al., 2015). These soils which have formed from the accumulation of
8 volcanic ash in flat valley bottoms and relatively low gradient slopes in combination with the
9 cold-humid climate have resulted in black, humic, and acid soils rich in organic matter
10 content with low bulk density and high water storage capacity (Quichimbo et al., 2012). The
11 organic fraction of the Histosol soils corresponds to an H horizon (median depth 76.5 cm);
12 while in the Andosol soils it corresponds to an Ah horizon (median depth 40cm). The mineral
13 fraction of both soils corresponds to a C horizon (median depth of 31 cm in the Histosols and
14 40 cm in the Andosols). A complete description of soil properties can be found in Mosquera
15 et al. (2015) and Quichimbo et al. (2012). Vegetation coverage is highly correlated with the
16 soil type. Cushion plants (such as *Plantago rigida*, *Xenophyllum humile*, *Azorella spp.*) grow
17 primarily in Histosols, while tussock grass (mainly *Calamagrostis* sp.) (Ramsay and Oxley,
18 1997; Sklenar and Jorgensen, 1999) grow in Andosols.

19 **2.2 Hydrometric information**

20 Discharge and precipitation were continuously monitored since October 2010. A nested
21 monitoring network was used to measure discharge. The network consisted of seven tributary
22 catchments (M1 to M7) draining to the outlet of the basin (M8). Catchments M1 to M6
23 comprise the main stream network draining towards the outlet of the Zhuruca y basin (M8),
24 whereas catchment M7 is a small catchment originated from a ponded wetland at a flat hilltop
25 (Figure 1). V-notch weirs were constructed to measure discharge at the outlet of the
26 tributaries M1-M7 and a rectangular weir at the outlet of the basin M8. Each catchment was
27 instrumented with pressure transducers with a precision of ± 5 mm. Water levels were
28 recorded at a 5-minute resolution, and transformed into discharge using the Kindsvater-Shen



1 relationship (U.S. Bureau of Reclamation, 2001). The discharge equations were calibrated by
2 applying the constant rate salt dissolution technique (Moore, 2004). Precipitation was
3 recorded using tipping buckets with a resolution of 0.2 mm at two stations located at 3780 and
4 3700 m a.s.l. (Figure 1).

5 **2.3 Collection and analysis of water stable isotopic and electrical conductivity** 6 **data**

7 We used a three-year record (May 2011 – May 2014) of ^{18}O and ^2H isotopic compositions of
8 water samples collected in precipitation and streamflow. Data were collected at different
9 resolutions, from event-based to biweekly, given logistic constraints and opportunities.
10 Higher resolution data were aggregated to biweekly using precipitation amount weighted
11 means for record consistency. The same nested monitoring network used for measuring
12 discharge was implemented for measuring stable isotopes in streamflow (i.e., seven tributary
13 catchments M1 to M7 draining towards M8 at the outlet of the basin). Water samples in
14 precipitation were collected using two rain collectors located at 3780 and 3700 m a.s.l. Each
15 collector consisted of a circular funnel and a polypropylene bottle covered with aluminum
16 foil. Evaporation was prevented by placing a plastic sphere (4 cm diameter) in the funnel and
17 a layer of 0.5 cm mineral oil within the polypropylene bottle. Due to the sampling procedure
18 and the local climate, kinetic fractionation by evaporation can be neglected and hence both
19 stable isotopes yield the same results (Mosquera et al., In review). Therefore only the results
20 using the isotopic composition of ^{18}O are reported. Rainwater samples are cumulative
21 representations of the isotopic signature between sampling dates while stream grab water
22 samples represent discrete points in time. The collected water samples were stored in 2 ml
23 amber glass bottles, covered with parafilm, and kept away from the sunlight to prevent
24 fractionation by evaporation as recommended by the International Atomic Energy Agency
25 (Mook, 2000). The isotopic composition of the water samples was measured using a cavity
26 ring-down spectrometer L1102-i (Picarro, USA) with a 0.5‰ precision for deuterium (^2H)
27 and 0.1‰ precision for oxygen-18 (^{18}O). Isotopic concentrations are presented in the δ
28 notation and expressed in per mill (‰) according to the Vienna Standard Mean Ocean Water
29 (V-SMOW) (Craig, 1961).



1 Electrical conductivity (EC) was measured directly instream simultaneously with the water
 2 isotopic data starting in 2012, the second year of the monitoring period. EC was measured
 3 using the digital conductivity sensor Tetracon 925 (WTW, Germany) with a precision of \pm
 4 0.5%.

5 **2.4 Mean transit time modeling and transit time distributions**

6 Mean transit time (MTT) was estimated using an inverse solution to the lumped parameter
 7 model approach (Amin and Campana, 1996; Maloszewski and Zuber, 1982), which seeks for
 8 the parameter set of the model that best describes the hydrologic system represented by a
 9 predefined transit time distribution (TTD) function (Maloszewski and Zuber, 1996). The TTD
 10 describes the transition of an input signal (e.g., precipitation, snow) of tracer (e.g., $\delta^{18}\text{O}$, $\delta^2\text{H}$)
 11 to the signal at an outlet point (e.g., groundwater, streamflow) resulting from the subsurface
 12 transport of water molecules within a catchment. Mathematically the TTD is described by a
 13 convolution integral that transforms the input signal (δ_{in}) into an output signal (δ_{out}),
 14 considering a time lag between both signals ($t - \tau$) through a transfer function
 15 (TTDs or $g(\tau)$) describing the subsurface transport of tracer as follows:

$$16 \quad \delta_{out}(t) = \int_0^{\infty} g(\tau) \delta_{in}(t - \tau) d\tau \quad (1)$$

17 where τ is the integration variable representing the MTT of the tracer. A more robust
 18 approximation weights the isotopic concentration of the input by considering recharge mass
 19 variation ($w(\tau)$) so that the outflow composition reflects the mass flux leaving the catchment:

$$20 \quad \delta_{out}(t) = \frac{\int_0^{\infty} g(\tau) w(t - \tau) \delta_{in}(t - \tau) d\tau}{\int_0^{\infty} g(\tau) w(t - \tau) d\tau} \quad (2)$$

21 where $w(t - \tau)$ can be described in terms of rainfall magnitude, intensity, or effective
 22 precipitation (McGuire and McDonnell, 2006). Precipitation intensity was used to volume
 23 weight the isotopic composition of precipitation in our study. Recharge was represented by
 24 the rainfall isotopic composition weighted by precipitation rate and accounted for relatively



1 small recharge (i.e., lower precipitation inputs) during the less wet months (August and
2 September).

3 MTT (τ in Eqs. 1 and 2) was estimated by adjusting the response function or TTD to fit the
4 measured and simulated stream water isotopic composition. Five TTDs were considered to
5 investigate which better describes the subsurface transport of water molecules in the Zhurucay
6 basin. We used the exponential model (EM), exponential-piston flow model (EPM), the
7 dispersion model (DM) (Małozzewski and Zuber, 1982), the gamma model (GM) (Kirchner et
8 al., 2000), and the two parallel linear reservoir model (TPLR) (Weiler et al., 2003). Each
9 model is briefly described below and Table 1 summarizes their equations, fitting parameters,
10 and the range of initial parameters used in this study.

11 The EM represents a well-mixed system and assumes contributions from all flow paths. It
12 assumes a relatively simple transition of the tracer towards the stream network. The EPM is
13 an extension of the EM in which a delay in the shortest flow paths is assumed by the piston
14 flow portion of the system. In addition to the MTT, it has an additional fitting parameter (η),
15 which represents the ratio of the total volume to the volume represented by the exponential
16 distribution. The DM arises from the solution of the one-dimensional advection-dispersion
17 equation (Kreft and Zuber, 1978) and assumes that there is influence of hydrodynamic
18 dispersion in the system's flow paths. It also has two fitting parameters, the MTT and the
19 dispersion parameter (Dp), which relates to the tracer transport process. The GM is a more
20 flexible and general version of the exponential model in which the product of two parameters
21 provides an estimation of the MTT of the system. These parameters are the shape parameter
22 (α) and the scale parameter (β) (Kirchner et al., 2000). The TPLR represents two parallel
23 reservoirs each one represented by a single exponential distribution. It has three fitting
24 parameters, the MTT of the slow (MTT_s) and fast (MTT_f) reservoirs and a parameter
25 representing the fraction of each of them with respect to total flow (φ) (Weiler et al., 2003).

26 The MTT approach bases on the following assumptions: 1) the solute concentration is
27 conservative (i.e., the tracer does not react with other elements present in the system); 2) the
28 tracer concentration is measured in flux mode; 3) the tracer enters the system only once and



1 uniformly; 4) a representative tracer input can be identified; 5) transport of solute is one-
2 dimensional and represented by a single TTD; and 6) there is a uniform storage of water
3 within the catchment (i.e., steady state of the flow in the system) (Małoszewski and Zuber,
4 1982). The steady-state assumption is valid for humid environments during specific flow
5 characteristics (i.e., baseflow) (McGuire et al., 2002). In order to comply with the latter
6 assumption, streamflow water samples collected during extreme rainfall events were excluded
7 for the MTT simulations (McGuire and McDonnell, 2006; Muñoz-Villers et al., 2015). To
8 obtain more stable results, we looped the available three years of isotopic data ten times
9 during calibration in order to extend the data series for 30 years as a warm-up period
10 following Hrachowitz et al. (2011) and Timbe et al. (2014).

11 **2.5 Model performance and uncertainty analysis**

12 The model performance was evaluated using the Kling–Gupta efficiency coefficient (KGE)
13 (Gupta et al., 2009). KGE ranges from $-\infty$ to 1, where unity indicates an ideal optimization.
14 KGE can be viewed from a multi-objective perspective because it accounts for correlation
15 (i.e., balancing dynamics, r), variability error (γ), and bias error (β) within a single objective
16 function. The efficiency is mathematically represented by the Euclidean distance (ED) in each
17 of the three dimensions (r , γ , and β) to an ideal point where all of them are maximized (i.e.,
18 where ideally the three factors are set to one). Efficiencies lower than 0.45 were considered
19 poor predictions (Timbe et al., 2014).

20 Depending on the TTD function used, 1 to 3 parameters were fitted during the simulations.
21 Each model was first run 10,000 times within a wide range of parameter values (Table 1).
22 Once a parameter value that yielded the best KGE was clearly identified, the model was run
23 again until obtaining 10,000 behavioral solutions (i.e., solutions corresponding to at least 95%
24 of the highest KGE) (Timbe et al., 2014) and their 5 and 95% limit bounds (i.e., 90%
25 confidence interval) were estimated using the Generalized Likelihood Uncertainty Estimation
26 methodology (GLUE) (Beven and Binley, 1992). In addition, the measure of identification
27 (MI) (Segura et al., 2012) was calculated as a metric of the model parameter identifiability.
28 The MI is defined as the ratio between the behavioral parameters range to the initial range and
29 indicates how well a parameter is identified. This metric is expressed as a percentage and by



1 definition, the smaller the value, the better the parameter identifiability. We considered a
2 parameter is well-identified if its MI is lower than 10%. The best model describing the
3 hydrologic conditions of the system was selected using the following criteria: 1) best
4 goodness of fit using the KGE criterion, 2) results that yielded the lower uncertainty
5 estimations, and 3) higher parameter identifiability using the MI criterion.

6 **2.6 Correlation analysis of MTT and catchment characteristics**

7 We used linear regression to investigate relations between landscape characteristics and
8 hydrological behavior with the MTT of the catchments. For this analysis, we included the
9 catchments which comprise the main drainage network (i.e., catchments M1 to M6) and the
10 catchment outlet (M8) given that they possess comparable hydrogeological and
11 geomorphological characteristics. That is, catchments situated at the valley bottom have well-
12 defined interconnections between wetlands in the riparian areas and the surrounding Andosol
13 soils at the slopes. Catchment M7 on the other hand, is located at a flat hilltop at the outlet of
14 a wetland area which remains ponded throughout the year. The geomorphology of this
15 concave (lagoon shaped) structure and its ponded eutrophic condition has allowed for the
16 hydrologic processes to majorly occur in the shallowest ponded portion of the water directly
17 connected to the stream network (with little influence of the most likely immobile water
18 which remains stored in the deeper soil fraction) (Mosquera et al., In review). Therefore, its
19 hydrological response is not comparable to the other catchments where hydrologic processes
20 mainly occur in the soils and consequently was excluded from the regression analysis.
21 Statistical significance of the correlations was tested using the F-test at a 95% confidence
22 level (i.e., $p < 0.05$).

23 The landscape and hydrometric variables tested for correlation were obtained from previous
24 studies at the site (Mosquera et al., 2015) and from detailed soil, vegetation, and topographic
25 information provided by INV Metals. The landscape features considered were: soil type,
26 vegetation, geology, catchment size, slope, flow path length and gradient, and topographic
27 wetness index (TWI) (Beven and Kirkby, 1979) (Table 2). The hydrometric variables
28 considered were: annual runoff, annual precipitation, runoff coefficient, and streamflow rates



1 (Table 3). Weekly collected EC for three years (June 2012-June 2015) was averaged and also
2 tested for correlation with MTT.

3 **3 Results**

4 **3.1 Hydrologic and isotopic characterization in rainfall and streamflow**

5 Precipitation in the Zhurucay basin is evenly distributed throughout the year (Figure 2a),
6 except for two months with relatively lower precipitation inputs (i.e., August and September),
7 both accounting for less than 8% of total annual precipitation. The hydrograph at the outlet of
8 the basin (M8) also depicts a flashy response to precipitation inputs, even during these less
9 humid months (see zoom in Figure 2a). Similar behavior is observed at all catchments.
10 Spatially, annual precipitation (P) is evenly distributed across the basin with an average of
11 $1,275 \pm 9$ mm. Total annual runoff (Q) is spatially more heterogeneous, varying between 684
12 and 864 mm per year. Similarly, runoff coefficient (Q/P) shows relatively high spatial
13 variability between 0.55 and 0.68 (Table 3).

14 The $\delta^{18}\text{O}$ isotopic composition in rainfall is highly variable throughout the year (e.g., average
15 $-10.2 \pm 0.32\text{‰}$ at the upper station) (Figure 2b) and follows a seasonal pattern with
16 isotopically enriched values during highest precipitation rates (April-May), and isotopically
17 depleted values in the less humid period (August-September). The $\delta^{18}\text{O}$ isotopic composition
18 in streamflow collected during low flows on the other hand, is much more damped (average -
19 $10.0 \pm 0.06\text{‰}$, at M8) than the isotopic composition in precipitation (Table 4). The
20 relationship between the $\delta^2\text{H}$ and $\delta^{18}\text{O}$ isotopic composition in all catchments plots between
21 the global and local relationships in rainfall (Figure 3). However, there are differences in the
22 regions where they plot within the relationship. M7 plots in a larger region than all of the
23 other catchments (golden diamonds). M3, and M4 (bluish open circles, subgroup 1) plot lower
24 in the relationship than M1, M2, M5, M6, and M8 (reddish crosses, subgroup 2).

25 **3.2 Model selection and mean transit time evaluation**

26 In order to identify the TTD best suitable to describe the hydrologic system in the Zhurucay
27 basin, we tested and evaluated the performance of all TTDs at all catchments (only results for



1 M8, the basin outlet, are shown for brevity; however similar results were obtained for the rest
2 of the catchments). The MTTs for the best performing TTD for all catchments will be further
3 discussed in detail.

4 All TTDs reproduce the $\delta^{18}\text{O}$ isotopic composition at the outlet of the basin (M8) with
5 efficiencies varying between 0.50 and 0.76, i.e., above the threshold of model acceptance
6 ($\text{KGE} > 0.45$) (Table 5). The more flexible models, GM and TPLR yield the highest
7 performances with KGEs of 0.75 and 0.76, respectively. The EM and the EPM yield similar
8 efficiencies ($\text{KGE} = 0.63$), while the DM yields the lowest efficiency among all ($\text{KGE} =$
9 0.50). The models associated with the highest KGEs yield the highest uncertainty bounds
10 according to their threshold of behavioral solutions, likely explained by an inverse relation
11 between the number of fitting parameters in a given model and the span of the confidence
12 bands (Figure 4).

13 The models' parameter identification analysis indicates that even though the TPLR model
14 yields the highest KGE, the level of identification of its parameters is the poorest (Figure 5).
15 The identification metric (IM, i.e., the ratio of behavioral parameter range to the initial
16 parameter range, Table 5) yields high values for all parameters for the TPLR model (MIs
17 ranges between 29% and 85%). For the EPM, DM, and GM models one parameter is well
18 identified (MIs $< 10\%$), while the others show higher MI values. The MI for the single
19 parameter that defines the EM is very strong (MI = 2%). This coupled analysis of model
20 efficiency and parameter identifiability indicates that although models with a higher number
21 of fitting parameters provide higher efficiencies, their parameters are more uncertain.

22 Taking into account both, the highest goodness of fit provided by a model and the
23 identifiability of its parameters, the EM is the model that best describes the temporal
24 variability of the $\delta^{18}\text{O}$ isotopic composition across the Zhurucay basin. Interpretation of
25 hydrologic processes is not feasible for all of the other models, as a result of the interplay
26 between different sets of poorly identified parameters.

27 The MTT probability density functions (PDFs, which indicate the distribution of MTTs in the
28 hydrologic system, Figure 6a) and cumulative density functions (CDFs, which express the
29 tracer “mass recovery from an instantaneous, uniform tracer mass addition”, McGuire et al.,



1 2005, Figure 6b) for each of the models show that the EM and the EPM are clearly dominated
2 by short MTTs, indicating a prevalence of short and/or very rapid flow paths of water in the
3 subsurface. On the contrary, the other models depict a dominance of longer MTTs as
4 evidenced by long flattened tails at the end of their PDFs. In a system where the hydrology
5 appears to be dominated by shallow subsurface flow, such as the Zhurucay basin (Mosquera
6 et al., In review), long transit times are unlikely to occur. Therefore, the dominance of short
7 MTTs of the EM and EPM linked to short flow paths of water are more suitable to represent
8 the subsurface transport of water in these páramo soils. However, the η proportional
9 parameter (the ratio of the total volume to the volume represented by exponential distribution)
10 of the EPM model is poorly identified. Thus, the EM is preferred to describe the hydrologic
11 conditions in Zhurucay basin. The EM was also found to describe the subsurface transport of
12 water of stream water in another volcanic soil dominated catchments in eastern Mexico
13 (Muñoz-Villers et al., 2015).

14 Hydrologically speaking, the EM represents a well-mixed reservoir with relatively simple
15 transition of the water (i.e., tracer) in the subsurface towards the stream network. Since the
16 isotopic composition of water stored in the Histosols (Andean wetlands) – which are
17 hydrologically connected to the drainage network – is homogeneous throughout the whole
18 profile of the organic and the shallow mineral horizon of this soil and there is no evidence of
19 significant groundwater contributions in the Zhurucay basin (Mosquera et al., In review), a
20 well-mixed reservoir is an appropriate assumption in the study site. In addition, as the
21 hydrologic system appears to be dominated by shallow subsurface flow within the porous
22 organic horizon of the páramo soils, a relatively simple transition of infiltrated precipitation
23 towards the catchment outlet is feasible. Therefore, this analysis, based on process
24 understanding and the characteristics of the physical system, in addition to the statistical
25 analysis of the hydrologic modeling, further support that the EM is the model that best
26 describes the transport of water across the Zhurucay basin.

27 Results of the EM for selected catchments with the longest (M3), intermediate (M6), and
28 lowest (M7) MTTs are shown in Figure 7 and statistics of the EM simulations at all
29 catchments are summarized in Table 6. The EM overcomes the modeling acceptance criterion
30 of $KGE > 0.45$ at all catchments with KGE values ranging between 0.48 and 0.84. The



1 longest MTTs are found in catchments M3 (0.73 years, 264 days) and M4 (0.67 years, 240
2 days) and the shortest at M7 (0.15 years, 53 days). The MTT for the other catchments vary
3 within this range. On average, within the 90% confidence level for the catchments forming
4 the main drainage network (M1-M6 and M8), MTT estimations show small variations (25
5 days at the lower confidence bound and 35 days at the upper confidence bound) with small
6 standard deviation (4 days for the upper bound and 6 days for the lower bound). For
7 catchment M7, variations are even smaller (9 days at the lower confidence bound and 11 days
8 at the upper confidence bound). In addition, the model performs best for catchments with high
9 variability in their isotopic composition during the monitoring period. For instance, catchment
10 M3 (Figure 7a) shows the smallest amplitude in isotopic variation for the observed and
11 simulated data (Table 6), coupled with the lowest KGE (0.48) and the highest MTT. On the
12 other hand, catchment M7 (Figure 7c) shows the highest amplitude in isotopic variation for
13 the observed and simulated data, coupled with the highest KGE (0.84) and the shortest MTT.
14 Similarly, catchment M6 (Figure 7b), which has a MTT shorter than the one in M3 and longer
15 than the one in M7, has an amplitude and KGE varying between the ones in M3 and M7. The
16 Monte Carlo simulations for the fitted parameter MTT (Figure 7) clearly depict how the MTT
17 which yield the highest KGE in each catchment decreases as the variation in their isotopic
18 composition increases as described above. Results from all the catchments are also described
19 by this trend.

20 The PDFs of the catchments (not shown for brevity) exhibit a dominance of relatively short
21 MTTs in the hydrology of the Zhurucay basin. The CDFs depict that the tracer is completely
22 recovered in all catchments at around 80 biweeks, except for M7, where the tracers is even
23 more rapidly recovered (~ 19 biweeks). As we used a stable isotopic record of 78 weeks (3
24 years), these results indicate that a three years record of tracer data is enough to estimate the
25 MTT of waters using the LPM approach in the páramo basin of the Zhurucay observatory.

26 **3.3 Correlations of Mean Transit Time with landscape and hydrometric** 27 **variables**

28 Correlation analysis showed no statistically significant correlations (p-values > 0.05) with
29 landscape features and hydrometric variables of the nested monitoring system when all



1 catchments were included. This lack of correlation is likely related to the previously reported
2 distinct responsiveness of catchment M7 to precipitation inputs due to its different
3 geomorphology (i.e., ponded eutrophized wetland disconnected from the slopes) and
4 catchments M3 and M4 (Figure 1) driven by a spring water contribution during low flow
5 generation. Although in general, groundwater contributions to discharge seem to be minimal
6 and geology has not been found to directly control the hydrology in this páramo ecosystem
7 (Mosquera et al., 2015), the existence of this shallow spring sourced at the interface between
8 the soil mineral horizon and the shallow bedrock upstream the outlet of M3 and M4 –
9 favoring the generation of higher low flows (Mosquera et al., In review) and increasing MTTs
10 in these catchments – indicates that geology (fractures in the shallow bedrock) influence the
11 hydrology of these small headwater catchments; thus, masking relationships between
12 landscape features and MTT of the whole system. Therefore, we tested the MTT correlations
13 without including these small catchments (M3 and M4) and M7 (subgroup 2). The reanalysis
14 with the modified data set revealed significant relations of MTT with topographical indexes
15 (Figure 8). The relations between MTT and average slope (Figure 8a, $R^2 = 0.78$ and $p =$
16 0.047) and percent area having slopes in the range 20%-40% are negative (Figure 8b, $R^2 =$
17 0.90 , $p = 0.015$). Conversely the relation between the percent area having slopes 0%-20% and
18 MTT is positive ($R^2 = 0.85$, $p = 0.026$).

19 The regression analysis including all catchments also showed that mean electrical
20 conductivity (MEC) of the waters explains 89% ($p < 0.001$) of the catchments' MTT
21 variability (Figure 9). Streams with higher MEC have longer MTTs. No significant
22 correlations (p -values > 0.05) between MTT and vegetation, soil types, geology, flow path
23 length, and topographic wetness index were found (Table 7).

24 **4 Discussion**

25 **4.1 General hydrometric and isotopic characterization**

26 The rainfall-runoff process evidences a rapid response of discharge to precipitation inputs in
27 the Zhurucay basin. This rapid response occurs even during the less humid periods (August-
28 September) in which relatively small rainfall events result in peak flow generation (Figure



1 2a). This high responsiveness results from the combined effect of the relatively uniform
2 distribution of precipitation year-round – common in tropical regions – and the unique
3 properties of the Histosol soils or Andean wetlands located near the streams. The high storage
4 capacity of wetlands was also highlighted by (Roa-García and Weiler, 2010) after the
5 comparison of three paired catchments in the growing coffee region of Colombia at lower
6 elevations (2000-2200 m a.s.l.). Similarly, Histosol soils in our study site are rich in organic
7 matter content (mean 86% by volume), allowing for high water storage capacity. In addition,
8 due to their relatively low saturated hydraulic conductivity ($0.72\text{-}1.55\text{ cm h}^{-1}$), these soils
9 remain near saturation throughout the year. These factors, in combination with the local
10 climate, allow páramo soils to regulate and maintain a sustained discharge throughout the
11 year. Moreover, as these processes occur in the shallow organic horizon of the soils, the
12 hydrology of the Zhurucay basin páramo ecosystem is dominated by shallow subsurface water
13 flow. This is supported by the similar isotopic composition between streams and soil waters in
14 the organic layer of the Histosols in the Zhurucay basin (Mosquera et al., In review).

15 The $\delta^{18}\text{O}$ isotopic composition of stream waters is damped and lagged with respect to that of
16 precipitation. Nevertheless, streamflow samples in the Zhurucay basin still reflect the
17 variability of the $\delta^{18}\text{O}$ composition of rainfall (Figure 2b), as expected in a system dominated
18 by shallow subsurface flow. The relationship between the $\delta^2\text{H}$ and $\delta^{18}\text{O}$ isotopic composition
19 in rainfall (LMWL) and streamflow indicates no isotopic fractionation by evaporation in local
20 precipitation and streamflow (see Mosquera et al., In review for details). Differences in the
21 region where catchments plot within this relationship indicate that they are differently
22 influenced by precipitation. M7, located at the outlet of a wetland that remains constantly
23 ponded, shows a faster response to rainfall, most likely as a result of the rapid mixing of
24 rainfall water with the shallow water moving in the organic horizon of the soils and the
25 ponded water above it. All of the other catchments show considerably less influence of
26 rainfall, although M3 and M4 (subgroup 1) show depleted values than M1, M2, M5, M6, and
27 M8 (subgroup 2). The latter most likely reflecting a small contribution from a small shallow
28 spring source to subgroup 1 (Mosquera et al., 2015).



1 **4.2 What is the MTT of stream waters?**

2 The high performance ($KGE > 0.48$) of the exponential model (EM) and its strong parameter
3 identification (Table 6) indicate that this model best mimics the subsurface transport of water
4 in all catchments within the Zhurucaiy basin (Figure 7). Nevertheless, the model captures
5 some particularities in the functioning of each catchment. For instance, results indicate
6 relatively long MTTs in two of the headwater catchments, M3 and M4 (0.73 and 0.67 years,
7 respectively). This results from a shallow spring water contribution to these catchments
8 during low flow generation (Mosquera et al., 2015). The model seems to capture the effect of
9 the shallow spring contribution by yielding the longest MTTs estimations in these catchments,
10 and an intrinsic influence of geology on MTT variability. In addition, the performance of the
11 model in these two catchments is the lowest within the basin. The latter most likely because
12 of less efficient mixing of water due to the influence of the spring water source; suggesting
13 that this effect is also captured by the model which assumes a well-mixed reservoir. In this
14 sense, it seemed logic to consider that another model representing an additional slow reservoir
15 (e.g., TPLR or GM) could have better represented the subsurface movement of water in these
16 catchments. Nevertheless, our results suggest that the contribution from this additional water
17 source is small and an additional reservoir is not well distinguished by these TTDs as their
18 parameters are not well identified. Recently, Muñoz-Villers et al. (2015) also identified the
19 EM as the model that best mimics subsurface flow in 7 of 12 nested catchments underlain by
20 volcanic soils (Andosols) in a TMCF located in Veracruz, Mexico. These authors estimated
21 even longer MTTs (1.2-2.2 years) due to deeper groundwater contributions to discharge.

22 On the other end, M7, dominated by contribution from the shallowest part of the organic
23 horizon of the soils and the ponded fraction of water accumulated in a ponded wetland –
24 which is directly connected to the stream channel – presents the shortest MTT of all
25 catchments (0.15 years, 53 days), linked to the highest model performance. Our results
26 support the hypothesis that this catchment presents a shorter MTT, indicating that the ponded
27 condition of the wetland allows for a rapid and efficient mixture of precipitated water with
28 ponded water and water stored in and released from the shallow organic horizon of the soil.
29 The latter resulting in a rapid delivery of event (new) water to the stream; whereas water
30 stored deeper in the soil seems to remains mostly immobile with minimal influence in the



1 hydrology of the catchment. The well-mixing and simpler delivery of water to the stream is
2 also captured by the high model performance.

3 The MTTs estimated for the rest of the catchments lie in between these two extremes and
4 their values and efficiencies vary depending on the amplitude of the isotopic tracer variation,
5 with longer MTTs in catchments where the amplitude of the signal is more damped –
6 evidencing lower influence of precipitation and less efficient mixing with the soil storage –
7 and vice versa. The MTT in these catchments vary relatively little in comparison to the rest of
8 the catchments (0.43 to 0.53 years, 156 to 191 days). Overall, the MTTs are relatively short,
9 further supporting previous evidence that shallow subsurface flow dominates the hydrology of
10 the ecosystem.

11 In other tropical latitudes, MTTs higher than 300 days were found in three paired Colombian
12 catchments applying the TPLR model (Roa-García and Weiler, 2010). These basins show
13 higher MTTs than the catchments in the Zhurucay basin most likely as a result of the higher
14 development of the volcanic ash soils (> 10 m), which allow the water to be stored for longer
15 periods in the subsurface. MTTs of stream waters longer than two years were also found in a
16 tropical montane cloud forest (TMCF) in southern Ecuador (Timbe et al., 2014), evidencing
17 that differently from our findings, this lower elevation ecosystem is dominated by deep
18 groundwater contributions. Preliminary MTT estimations of stream water in another TMCF
19 biome located in central Mexico (Muñoz-Villers and McDonnell, 2012) yielded a MTT of
20 three years. Although the ecosystem is dominated by soils formed by volcanic ash
21 accumulation, as the páramo soils are, a combination of deeper hillslope soils (1.5-3 m depth)
22 with highly fractured and permeable geology allows for the formation of longer flow paths of
23 water and longer MTTs. Therefore, the relatively young and little weathered geology in the
24 Zhurucay basin allows for a dominance of shallow subsurface flows. The results of these
25 studies suggest that the particular shallow development of the rich organic soils with low
26 saturated hydraulic conductivities, in combination with an homogeneous and low permeable
27 geology provide the páramo basin of the Zhurucay River with a high water retention capacity,
28 and relatively long transit times and flow paths considering the little development of the
29 organic horizon of the soils. Hrachowitz et al. (2009b) reported MTT of stream water (135-
30 202 days) around the ones found in the Zhurucay basin catchments in a montane catchment in



1 Scotland dominated by peatland soils and relatively little weathering geology. Nevertheless,
2 the models which provided the best fit were the GM and the TPLR, as opposed to the EM in
3 our study site. As in the Zhurucay basin, these authors attributed this short transit time to the
4 dominance of ecohydrological processes occurring in the upper horizon of the peat soils.
5 Therefore, we can conclude that in these two ecosystems, located at different latitudes but
6 with similar hydroopedological conditions, the hydrology is dominated by shallow subsurface
7 flows. Nevertheless, the soils development of the shallow peaty soils in Scotland is lower (40
8 cm) in comparison to the soil development of the Histosols (80 cm) in the Zhurucay basin.
9 These factors, in combination with differences underlying geologies suggest that their overall
10 hydrologic functioning might differ as evidenced by different TTDs describing the subsurface
11 transport of solute.

12 **4.3 Controls on MTT variability**

13 We found significant correlations ($R^2 \geq 0.78$, $p < 0.05$) between catchment slope dependent
14 indexes and MTT using a subset of the main stream catchments (subgroup 2) (Table 7, Figure
15 8). Results of the correlation analysis indicate that 1) the higher the average slope of the
16 catchments, the shorter the MTT; 2) the higher the percent of area corresponding to slopes
17 between 0% and 20%, the longer the MTT; and 3) the higher the percent of area
18 corresponding to slopes between 20% and 40%, the shorter the MTT. These results indicate a
19 clear control of the catchments' slopes in the MTT of stream waters in the Zhurucay basin.
20 Locally, the same topographical features were found to control low flow generation.
21 Mosquera et al. (2015) attributed the latter to expected contributions from the water originated
22 in the slopes (Andosol soils) during low flow generation as a result of the gravitational
23 potential of the water that drains downslope from these soils. These authors also found that
24 wetlands (Histosols soils located near the streams) control the generation of moderate and
25 high flows. Although we did not find significant correlations with other landscape features,
26 vegetation shown expected trends in relation to MTT. That is, catchments with higher
27 proportion of cushion plants (wetlands) ($R^2 = 0.29$, $p = 0.35$) have longer MTTs and an
28 inverse relation with tussock grass vegetation ($R^2 = 0.31$, $p = 0.33$). In another tropical system
29 of catchments in Colombia, a catchment with higher areal proportion of wetlands was found



1 to prolong the MTT of stream waters, but appeared to reduce water yield (Roa-García et al.,
2 2011). Although these authors did not report the slope of the catchments, we can infer that the
3 catchment with the highest proportion of wetlands – as they form in flat areas – is also the
4 catchment with the lowest gradients. Therefore, their observations might result from the
5 combination of the deeper soil development (> 10 m) with high water retention capacity and
6 low saturated hydraulic conductivity, perhaps in combination with low slope gradients. This
7 would support the result of our study, where the catchments with the lower slopes and higher
8 proportion of wetlands present the longer MTTs.

9 In other latitudes, in 20 Scottish catchments with different geomorphologies and climate,
10 MTT variability was controlled by the areal proportion of peat soils and no influence of
11 catchments' slopes was found (Hrachowitz et al., 2009a). As such, and given the similarities
12 between these soils and our Histosol soils (Andean wetlands), we hypothesized the MTT
13 variability of streams to be controlled by the areal extent of wetlands. Even though we found
14 that MTT variability is rather majorly controlled by topography in our tropical alpine site, a
15 small trend of wetlands' cover to increase MTT was also identified. Although the later
16 relation is not statistically significant, the latter most likely results from the influence of
17 topography on Histosol soils (wetlands) formation, where the formation of this soil mainly
18 occurs in catchments with lower slopes where water accumulation is favored. This finding
19 indirectly suggests that wetlands influence MTT spatial variability to a lesser extent.
20 Therefore, it appears that although relatively similar processes control the ecohydrology of
21 both ecosystems, controls on MTT variability cannot be extended from one ecosystem to the
22 other. MTT variability was also found to be controlled by the proportion of wetlands in cold
23 snow dominate boreal catchments in Sweden for the MTT of spring snowmelt water (Lyon et
24 al., 2010). These authors attributed this effect to the formation of shallow ice acting as
25 impermeable barriers above the wetlands, and thus changing the flow paths of water.
26 Nevertheless, because of the different climate and geological features between their
27 catchments and ours, we did not find wetlands as major controls on MTT variability.
28 Other slope topographic indexes – e.g., flow path length (L), flow path gradient (G), and the
29 ratio between both (L/G) (e.g., McGuire et al., 2005; Tetzlaff et al., 2009) – have been
30 identified to control MTT variability in catchments in other latitudes. Although these



1 landscape features did not significantly explained MTT variability in the Zhurucay basin, the
2 L/G ratio was reported as the major control of MTT variability ($R^2 = 0.91$) in steep temperate
3 catchments in the central western Cascades of Oregon (McGuire et al., 2005), suggesting that
4 this relation “reflects the hydraulic driving force of catchment-scale transport (i.e., Darcy’s
5 law)”. Similarly to our study site, they also found average slope of these catchments to be one
6 of the most important individual controls on MTT, explaining 78% of the MTT variability.
7 Recently, topography was also identified as a major control on the MTT of 12 TMCF
8 catchments in eastern Mexico (Muñoz-Villers et al., 2015). Results from our these two studies
9 reflect that the integrated effect of catchment slope on MTT variation can be identified in
10 distinct geological and hydrogeological provinces. The latter also suggests that rather than
11 using a predictor which indicates more local effects of hydraulic force driving in the stream
12 channel (e.g., L/G), catchment slope might be a better measure to compare catchment
13 functioning as it integrates the hydrologic connectivity of hillslope, riparian, and stream areas.
14 The catchment slope topographic controls on MTT in the Zhurucay basin indicate that water
15 resides for a longer time in the hydrologic system of catchments having lower slope gradients.
16 These results also indicate that in catchments having higher areal proportions of low gradients
17 and lower areal proportions of steeper gradients coupled with higher wetlands coverage, water
18 resides longer in the shallow reservoir of the soils. Therefore, it is apparent that water stored
19 in the wetlands is released to the streams depending on the catchments’ topography. In
20 addition, the control of the proportion of steeper gradients in MTT variability also suggests
21 that the gravitational potential of water draining downslope in the Andosol soils also
22 indirectly influences the MTT of the streams. Overall, these results indicate that the high
23 storage capacity of the wetland soils (Histosols) located near the streams is not the only factor
24 providing páramo ecosystems with a high regulation capacity. Rather, it seems that the
25 interplay between the high storage capacity of the wetlands and the topography of the terrain
26 is what drives the extremely high water regulation capacity of this ecosystem. These
27 interpretations do not only make physical sense, but also add to our current process-based
28 understanding of páramo hydrology. In this shallow subsurface flow dominated system with a
29 high soil water retention capacity, it is clear that catchment topography is the factor driving
30 water movement. Without the interplay storage-slope, water would remain stored in the soils,



1 and perhaps the delivery of water towards the streams would be dominated by saturated
2 overland flow (SOF), affecting the regulation capacity of the ecosystem. Nevertheless, SOF
3 rarely occurs in the Zhurucay basin (Mosquera et al., 2015). Therefore, it is our interpretation
4 that the hydrology of this ecosystem is mainly dominated by two factors: 1) the high storage
5 capacity in the shallow organic horizon of the porous páramo soils and 2) the catchment
6 slope. Factor 1 driving the high water retention capacity and factor 2 controlling the high
7 regulation capacity of the ecosystem, and thus, maintaining a sustained delivery of water to
8 the streams along the year.

9 Mean electrical conductivity (MEC) was also found to be significantly correlated with the
10 MTT of the streams using all catchments of the nested system in the basin (Figure 9). The
11 regression analysis, showed strong correlation, with MEC increasing as the MTT of water
12 increases. As EC is an intrinsic property of water, due to the time it spends in contact with the
13 surrounding pore space, rather than a control on MTT variability, this result indicates that this
14 property might be used as a proxy to estimate MTT spatial variability. The well-defined
15 connection between MTT and MEC most likely resulting from the relatively homogenous
16 geology of the Zhurucay basin. To our knowledge, there are no studies that have identified
17 similar (or different) relations between MEC and MTT in other biomes.

18 Given that estimating MTT using isotope tracers and the LPM approach is financially
19 expensive due to the logistical set up of a monitoring network and the processes of data
20 collection and analysis, finding proxies (i.e., predictors) which allow inferring the MTT of
21 stream waters at lower operational costs is critical to improve water resources management. In
22 this sense, the strong relation between MEC and MTT indicates that MEC could be used as a
23 relatively inexpensive and directly measurable proxy for MTT in this wet Andean páramo
24 catchment. Therefore, although this result cannot be expanded beyond páramo areas, perhaps
25 not even beyond the study site, it seems that it is worth evaluating whether or not MEC can
26 infer MTT in other hydrologic systems. Nevertheless, one should be careful that EC
27 measurements can be relatively variable over time. As a result, a single measurement of EC is
28 most likely not enough to provide robust MTT estimates. Therefore, the longer the record of
29 EC measurements, the smallest the variability of MEC and the highest the robustness of MTT
30 estimates.



1 5 Conclusions

2 The MTT evaluation using a LPM indicated that the EM best describes the subsurface
3 transport of water in the basin. This result indicates efficient mixing in the high organic and
4 porous wet Andean páramo soils and a simple subsurface transition of rainfall water towards
5 the streams. MTT estimations showed relatively short MTTs of stream waters linked to
6 relatively short subsurface flow paths. Therefore, we confirm that the hydrologic system of
7 the tropical alpine biome of the Zhuruca y basin is dominated by shallow subsurface flow.
8 MTT estimations showed that catchment M7, located at a flat hilltop at the outlet of a wetland
9 which remains ponded year-round and disconnected from the slopes – most likely as a result
10 of the eutrophication of a lagoon – showed a particularly low MTT (0.15 yr – 53 days) in
11 relation to the MTT in all of the other catchments (0.40-73 yr, 156-250 days) in which the
12 morphology corresponds to U-shaped valleys, with the wetlands located at the valley bottoms
13 near the streams and connected to the slopes. Two headwater catchments, M3 and M4,
14 showed the longest MTT, related to a small contribution from a spring shallowly sourced.
15 These results indicate that in this páramo ecosystem, the geomorphology of the wetlands and
16 geology to a lesser extent, influence the responsiveness of the streams to precipitation inputs.
17 Correlation analysis between landscape variables and MTT indicates that MTT variability is
18 majorly explained by the slope of the catchments, and a related influence of vegetation to a
19 lesser extent. Catchments with the steepest average slopes and lower proportion of wetlands
20 have the shortest MTTs. The lack of significant correlations between the MTT of streams and
21 hydrological response variables (runoff coefficient and specific discharge rates) indicate that
22 neither water yield, nor streamflow rates control the time water resides in subsurface of the
23 páramo soils. These results indicate that the interplay between the high storage capacity of the
24 páramo soils and the slope of the catchments define the ecosystem's high regulation capacity.
25 Mean electrical conductivity (MEC) of stream waters – with the oldest waters presenting the
26 highest MECs – seems to be a promising proxy of MTT in system of catchments under
27 homogeneous geological conditions. Finally, we want to highlight the usefulness of a nested
28 monitoring system for acquiring better process-based hydrologic functioning understanding.
29 For instance, if M3, M4, and/or M7 catchments would not have been monitored, the influence
30 of geology and/or geomorphology on catchment hydrological response could not have been



1 identified and important information about the whole ecosystem functioning would remain
2 unknown.

3 **Acknowledgements**

4 The research was funded by the Central Research Office at the University of Cuenca (DIUC)
5 via the project “Desarrollo de indicadores eco-hidrológicos funcionales para evaluar la
6 influencia de las laderas y humedales en una cuenca de páramo húmedo”; and the Ecuadorian
7 National Secretariat of Higher Education, Science, Technology and Innovation (SENESCYT).
8 The authors express gratitude to INV Metals S.A. (Loma Larga Project) for the logistic
9 support. Special thanks to Alicia Correa for her fieldwork assistance and Irene Cardenas for
10 the laboratory analysis.
11



1 **References**

- 2 Amin, I. E. and Campana, M. E.: A general lumped parameter model for the interpretation of
3 tracer data and transit time calculation in hydrologic systems, *J. Hydrol.*, 179(1-4), 1–21,
4 doi:10.1016/0022-1694(95)02880-3, 1996.
- 5 Bethke, C. M. and Johnson, T. M.: Paradox of groundwater age: Correction, *Geology*, 30(4),
6 385–388, doi:10.1130/0091-7613(2002)030, 2002.
- 7 Beven, K. and Binley, A.: The future of distributed models: Model calibration and uncertainty
8 prediction, *Hydrol. Process.*, 6(3), 279–298, doi:10.1002/hyp.3360060305, 1992.
- 9 Beven, K. J. and Kirkby, M. J.: A physically based, variable contributing area model of basin
10 hydrology, *Hydrol. Sci. Bull.*, 24(1), 43–69, doi:10.1080/02626667909491834, 1979.
- 11 Broxton, P. D., Troch, P. A. and Lyon, S. W.: On the role of aspect to quantify water transit
12 times in small mountainous catchments, *Water Resour. Res.*, 45(8), n/a–n/a,
13 doi:10.1029/2008WR007438, 2009.
- 14 Célleri, R. and Feyen, J.: The Hydrology of Tropical Andean Ecosystems: Importance,
15 Knowledge Status, and Perspectives, *Mt. Res. Dev.*, 29(4), 350–355, doi:10.1659/mrd.00007,
16 2009.
- 17 Coltorti, M. and Ollier, C. .: Geomorphic and tectonic evolution of the Ecuadorian Andes,
18 *Geomorphology*, 32(1-2), 1–19, doi:10.1016/S0169-555X(99)00036-7, 2000.
- 19 Córdova, M., Carrillo-Rojas, G., Crespo, P., Wilcox, B. and Célleri, R.: Evaluation of the
20 Penman-Monteith (FAO 56 PM) Method for Calculating Reference Evapotranspiration Using
21 Limited Data, *Mt. Res. Dev.*, 35(3), 230–239, doi:10.1659/MRD-JOURNAL-D-14-0024.1,
22 2015.
- 23 Craig, H.: Standard for Reporting Concentrations of Deuterium and Oxygen-18 in Natural
24 Waters., *Science*, 133(3467), 1833–4, doi:10.1126/science.133.3467.1833, 1961.
- 25 Crespo, P., Bücker, A., Feyen, J., Vaché, K. B., Frede, H.-G. and Breuer, L.: Preliminary
26 evaluation of the runoff processes in a remote montane cloud forest basin using Mixing
27 Model Analysis and Mean Transit Time, *Hydrol. Process.*, 26(25), 3896–3910,
28 doi:10.1002/hyp.8382, 2012.
- 29 Crespo, P. J., Feyen, J., Buytaert, W., Bücker, A., Breuer, L., Frede, H.-G. and Ramírez, M.:



- 1 Identifying controls of the rainfall–runoff response of small catchments in the tropical Andes
2 (Ecuador), *J. Hydrol.*, 407(1-4), 164–174, doi:10.1016/j.jhydrol.2011.07.021, 2011.
- 3 Etcheverry, D. and Perrochet, P.: Direct simulation of groundwater transit-time distributions
4 using the reservoir theory, *Hydrogeol. J.*, 8(2), 200–208, doi:10.1007/s100400050006, 2000.
- 5 Freeze, R. A.: Role of subsurface flow in generating surface runoff: 2. Upstream source areas,
6 *Water Resour. Res.*, 8(5), 1272–1283, doi:10.1029/WR008i005p01272, 1972.
- 7 Goldsmith, G. R., Muñoz-Villers, L. E., Holwerda, F., McDonnell, J. J., Asbjornsen, H. and
8 Dawson, T. E.: Stable isotopes reveal linkages among ecohydrological processes in a
9 seasonally dry tropical montane cloud forest, *Ecohydrology*, 5(6), 779–790,
10 doi:10.1002/eco.268, 2012.
- 11 Goller, R., Wilcke, W., Leng, M. J., Tobschall, H. J., Wagner, K., Valarezo, C. and Zech, W.:
12 Tracing water paths through small catchments under a tropical montane rain forest in south
13 Ecuador by an oxygen isotope approach, *J. Hydrol.*, 308(1-4), 67–80,
14 doi:10.1016/j.jhydrol.2004.10.022, 2005.
- 15 Gupta, H. V., Kling, H., Yilmaz, K. K. and Martinez, G. F.: Decomposition of the mean
16 squared error and NSE performance criteria: Implications for improving hydrological
17 modelling, *J. Hydrol.*, 377(1-2), 80–91, doi:10.1016/j.jhydrol.2009.08.003, 2009.
- 18 Hewlett, J. D.: Soil moisture as a source of base flow from steep mountain watersheds, U.S.
19 Dept of Agriculture, Forest Service, Southeastern Forest Experiment Station, Asheville, N.C.,
20 1961.
- 21 Hrachowitz, M., Soulsby, C., Tetzlaff, D., Dawson, J. J. C. and Malcolm, I. A.:
22 Regionalization of transit time estimates in montane catchments by integrating landscape
23 controls, *Water Resour. Res.*, 45(5), n/a–n/a, doi:10.1029/2008WR007496, 2009a.
- 24 Hrachowitz, M., Soulsby, C., Tetzlaff, D., Dawson, J. J. C., Dunn, S. M. and Malcolm, I. A.:
25 Using long-term data sets to understand transit times in contrasting headwater catchments, *J.*
26 *Hydrol.*, 367(3-4), 237–248, doi:10.1016/j.jhydrol.2009.01.001, 2009b.
- 27 Hrachowitz, M., Soulsby, C., Tetzlaff, D. and Malcolm, I. A.: Sensitivity of mean transit time
28 estimates to model conditioning and data availability, *Hydrol. Process.*, 25(6), 980–990,
29 doi:10.1002/hyp.7922, 2011.



- 1 IUCN: High Andean Wetlands, Gland, Switzerland., 2002.
- 2 Kirchner, J. W., Feng, X. and Neal, C.: Fractal stream chemistry and its implications for
3 contaminant transport in catchments, *Nature*, 403(6769), 524–527, doi:10.1038/35000537,
4 2000.
- 5 Kreft, A. and Zuber, A.: On the physical meaning of the dispersion equation and its solutions
6 for different initial and boundary conditions, *Chem. Eng. Sci.*, 33(11), 1471–1480,
7 doi:10.1016/0009-2509(78)85196-3, 1978.
- 8 Lyon, S. W., Laudon, H., Seibert, J., Mörth, M., Tetzlaff, D. and Bishop, K. H.: Controls on
9 snowmelt water mean transit times in northern boreal catchments, *Hydrol. Process.*, 24(12),
10 1672–1684, doi:10.1002/hyp.7577, 2010.
- 11 Maloszewski, P. and Zuber, A.: Lumped parameter models for the interpretation of
12 environmental tracer data, in *Manual on Mathematical Models in Isotope Hydrogeology*.
13 *TECDOC-910.*, 1996.
- 14 Małoszewski, P. and Zuber, A.: Determining the turnover time of groundwater systems with
15 the aid of environmental tracers, *J. Hydrol.*, 57(3-4), 207–231, doi:10.1016/0022-
16 1694(82)90147-0, 1982.
- 17 McDonnell, J. J., McGuire, K., Aggarwal, P., Beven, K. J., Biondi, D., Destouni, G., Dunn,
18 S., James, A., Kirchner, J., Kraft, P., Lyon, S., Maloszewski, P., Newman, B., Pfister, L.,
19 Rinaldo, A., Rodhe, A., Sayama, T., Seibert, J., Solomon, K., Soulsby, C., Stewart, M.,
20 Tetzlaff, D., Tobin, C., Troch, P., Weiler, M., Western, A., Wörman, A. and Wrede, S.: How
21 old is streamwater? Open questions in catchment transit time conceptualization, modelling
22 and analysis, *Hydrol. Process.*, 24(12), 1745–1754, doi:10.1002/hyp.7796, 2010.
- 23 McGlynn, B. L. and McDonnell, J. J.: Quantifying the relative contributions of riparian and
24 hillslope zones to catchment runoff, *Water Resour. Res.*, 39(11), n/a–n/a,
25 doi:10.1029/2003WR002091, 2003.
- 26 McGuire, K. ., DeWalle, D. . and Gburek, W. .: Evaluation of mean residence time in
27 subsurface waters using oxygen-18 fluctuations during drought conditions in the mid-
28 Appalachians, *J. Hydrol.*, 261(1-4), 132–149, doi:10.1016/S0022-1694(02)00006-9, 2002.
- 29 McGuire, K. J. and McDonnell, J. J.: A review and evaluation of catchment transit time



- 1 modeling, *J. Hydrol.*, 330(3-4), 543–563, doi:10.1016/j.jhydrol.2006.04.020, 2006.
- 2 McGuire, K. J., McDonnell, J. J., Weiler, M., Kendall, C., McGlynn, B. L., Welker, J. M. and
3 Seibert, J.: The role of topography on catchment-scale water residence time, *Water Resour.*
4 *Res.*, 41(5), n/a–n/a, doi:10.1029/2004WR003657, 2005.
- 5 Mook, W. G.: Introduction: Theory, methods, review, in *Environmental Isotopes in the*
6 *Hydrological Cycle: Principles and Applications*, edited by W. G. Mook, IAEA and
7 UNESCO, Paris / Vienna., 2000.
- 8 Moore, R. D.: Introduction to salt dilution gauging for streamflow measurement Part 2:
9 Constant-rate injection, *Streamline Watershed Manag. Bull.*, 8(1), 11–15, 2004.
- 10 Mosquera, G. M., Lazo, P. X., Célleri, R., Wilcox, B. P. and Crespo, P.: Runoff from tropical
11 alpine grasslands increases with areal extent of wetlands, *CATENA*, 125, 120–128,
12 doi:10.1016/j.catena.2014.10.010, 2015.
- 13 Mosquera, G. M., Célleri, R., Lazo, P. X., Vaché, K. B. and Crespo, P. J.: Combined Isotopic
14 and Hydrometric Characterization towards Ecohydrological Processes Conceptualization in a
15 High-Elevation Tropical Ecosystem, *Hydrol. Process.*, In review
- 16 Muñoz-Villers, L. E. and McDonnell, J. J.: Runoff generation in a steep, tropical montane
17 cloud forest catchment on permeable volcanic substrate, *Water Resour. Res.*, 48(9), n/a–n/a,
18 doi:10.1029/2011WR011316, 2012.
- 19 Muñoz-Villers, L. E., Geissert, D. R., Holwerda, F. and McDonnell, J. J.: Factors influencing
20 stream water transit times in tropical montane watersheds, *Hydrol. Earth Syst. Sci. Discuss.*,
21 12(10), 10975–11011, doi:10.5194/hessd-12-10975-2015, 2015.
- 22 Padrón, R. S., Wilcox, B. P., Crespo, P. and Célleri, R.: Rainfall in the Andean Páramo: New
23 Insights from High-Resolution Monitoring in Southern Ecuador, *J. Hydrometeorol.*, 16(3),
24 985–996, doi:10.1175/JHM-D-14-0135.1, 2015.
- 25 Penna, D., Tromp-van Meerveld, H. J., Gobbi, A., Borga, M. and Dalla Fontana, G.: The
26 influence of soil moisture on threshold runoff generation processes in an alpine headwater
27 catchment, *Hydrol. Earth Syst. Sci.*, 15(3), 689–702, doi:10.5194/hess-15-689-2011, 2011.
- 28 Pratt, W. T., Figueroa, J. F. and Flores, B. G.: Geology and Mineralization of the Area
29 between 3 and 48S. Western Cordillera, Ecuador. Open File Report, WCr97r28. British



- 1 Geological Survey., 1997.
- 2 Quichimbo, P., Tenorio, G., Borja, P., Cárdenas, I., Crespo, P. and Célleri, R.: Efectos sobre
3 las propiedades físicas y químicas de los suelos por el cambio de la cobertura vegetal y uso
4 del suelo: páramo de Quimsacocha al sur del Ecuador., *Suelos Ecuatoriales*, 42(2), 138–153,
5 2012.
- 6 Ramsay, P. M. and Oxley, E. R. B.: The growth form composition of plant communities in
7 the ecuadorian páramos, *Plant Ecol.*, 131(2), 173–192, doi:10.1023/A:1009796224479, 1997.
- 8 Roa-García, M. C. and Weiler, M.: Integrated response and transit time distributions of
9 watersheds by combining hydrograph separation and long-term transit time modeling, *Hydrol.*
10 *Earth Syst. Sci.*, 14(8), 1537–1549, doi:10.5194/hess-14-1537-2010, 2010.
- 11 Roa-García, M. C., Brown, S., Schreier, H. and Lavkulich, L. M.: The role of land use and
12 soils in regulating water flow in small headwater catchments of the Andes, *Water Resour.*
13 *Res.*, 47(5), W05510, doi:10.1029/2010WR009582, 2011.
- 14 Rodhe, A., Nyberg, L. and Bishop, K.: Transit Times for Water in a Small Till Catchment
15 from a Step Shift in the Oxygen 18 Content of the Water Input, *Water Resour. Res.*, 32(12),
16 3497–3511, doi:10.1029/95WR01806, 1996.
- 17 Segura, C., James, A. L., Lazzati, D. and Roulet, N. T.: Scaling relationships for event water
18 contributions and transit times in small-forested catchments in Eastern Quebec, *Water Resour.*
19 *Res.*, 48(7), n/a–n/a, doi:10.1029/2012WR011890, 2012.
- 20 Sklenar, P. and Jorgensen, P. M.: Distribution patterns of paramo plants in Ecuador, *J.*
21 *Biogeogr.*, 26(4), 681–691, doi:10.1046/j.1365-2699.1999.00324.x, 1999.
- 22 Soulsby, C., Tetzlaff, D., Rodgers, P., Dunn, S. and Waldron, S.: Runoff processes, stream
23 water residence times and controlling landscape characteristics in a mesoscale catchment: An
24 initial evaluation, *J. Hydrol.*, 325(1-4), 197–221, doi:10.1016/j.jhydrol.2005.10.024, 2006.
- 25 Tetzlaff, D., Seibert, J., McGuire, K. J., Laudon, H., Burns, D. A., Dunn, S. M. and Soulsby,
26 C.: How does landscape structure influence catchment transit time across different
27 geomorphic provinces?, *Hydrol. Process.*, 23(6), 945–953, doi:10.1002/hyp.7240, 2009.
- 28 Tetzlaff, D., Carey, S. K., Laudon, H. and McGuire, K.: Catchment processes and
29 heterogeneity at multiple scales-benchmarking observations, conceptualization and



- 1 prediction, *Hydrol. Process.*, 24(16), 2203–2208, doi:10.1002/hyp.7784, 2010.
- 2 Tetzlaff, D., Al-Rawas, G., Blöschl, G., Carey, S. K., Fan, Y., Hrachowitz, M., Kirnbauer, R.,
3 Jewitt, G., Laudon, H., McGuire, K. J., Sayama, T., Soulsby, C., Zehe, E. and Wagener, T.:
4 Process realism: Flow paths and storage., in *Runoff prediction in ungauged basins: Synthesis*
5 *across processes, places and scales*, edited by G. Blösch, M. Sivapalan, T. Wagener, A.
6 Viglione, and H. Savenije, pp. 53–69, Cambridge University Press, Cambridge, UK;, 2013.
- 7 Tetzlaff, D., Birkel, C., Dick, J., Geris, J. and Soulsby, C.: Storage dynamics in
8 hydrogeological units control hillslope connectivity, runoff generation, and the evolution of
9 catchment transit time distributions., *Water Resour. Res.*, 50(2), 969–985,
10 doi:10.1002/2013WR014147, 2014.
- 11 Timbe, E., Windhorst, D., Crespo, P., Frede, H.-G., Feyen, J. and Breuer, L.: Understanding
12 uncertainties when inferring mean transit times of water trough tracer-based lumped-
13 parameter models in Andean tropical montane cloud forest catchments, *Hydrol. Earth Syst.*
14 *Sci.*, 18(4), 1503–1523, doi:10.5194/hess-18-1503-2014, 2014.
- 15 U.S. Bureau of Reclamation: *Water Measurement Manual*, Washington DC., 2001.
- 16 Vimeux, F., Tremoy, G., Risi, C. and Gallaire, R.: A strong control of the South American
17 SeeSaw on the intra-seasonal variability of the isotopic composition of precipitation in the
18 Bolivian Andes, *Earth Planet. Sci. Lett.*, 307(1-2), 47–58 [online] Available from:
19 <http://www.documentation.ird.fr/hor/fdi:010053700> (Accessed 3 December 2015), 2011.
- 20 Weiler, M., McGlynn, B. L., McGuire, K. J. and McDonnell, J. J.: How does rainfall become
21 runoff? A combined tracer and runoff transfer function approach, *Water Resour. Res.*, 39(11),
22 n/a–n/a, doi:10.1029/2003WR002331, 2003.
- 23 Windhorst, D., Waltz, T., Timbe, E., Frede, H.-G. and Breuer, L.: Impact of elevation and
24 weather patterns on the isotopic composition of precipitation in a tropical montane rainforest,
25 *Hydrol. Earth Syst. Sci.*, 17(1), 409–419, doi:10.5194/hess-17-409-2013, 2013.
- 26



- 1 Table 1. Models considered to describe mean transit time (MTT) of stream waters in the study
2 area and their transit time distribution (TTD) functions, parameters, and range of initial
3 parameters.

Model	Transit time distribution (g(τ))	Parameter(s) range
Exponential model (EM)	$\frac{1}{\tau} \exp\left(-\frac{t}{\tau}\right)$	τ [0 – 200]
Exponential-piston model (EPM)	$\frac{\eta}{\tau} \exp\left(-\frac{t \cdot \eta}{\tau} + \eta - 1\right)$ for $t \geq \tau(1 - \eta^{-1})$	τ [0 – 200] η [0.5 – 4]
Dispersion model (DM)	$\left(\frac{4\pi D_p t}{\tau}\right)^{-1/2} t^{-1} \exp\left[-\left(1 - \frac{t}{\tau}\right)^2 \left(\frac{\tau}{4D_p t}\right)\right]$	τ [0 – 200] D_p [0.5 – 4]
Gamma model (GM)	$\frac{\tau^{\alpha-1}}{\beta^\alpha \Gamma(\alpha)} \exp^{-\tau/\beta}$	τ [0 – 200] α [0.5 – 4] $\beta = \tau/\alpha$
Two parallel linear reservoir (TPLR)	$\frac{\varphi}{\tau_f} \exp\left(-\frac{t}{\tau_f}\right) + \frac{1-\varphi}{\tau_s} \exp\left(-\frac{t}{\tau_s}\right)$	τ_s [0 – 200] τ_f [0 – 20] φ [0 – 1]

- 4 τ = tracer's mean transit time (MTT) in biweeks; η = parameter that indicates the percentage
5 of contribution of each flow type; D_p = dispersion parameter; τ_f and τ_s = transit time of fast
6 and slow flows in biweeks; φ = flow partition parameter between fast and slow flow
7 reservoirs.



1

Table 2. Main landscape characteristics of the monitored catchments.

Catchment	Area (km ²)	Altitude (m a.s.l)	Distribution of soil types ^a (%)			Vegetation cover ^b (%)			Topography ^c (%)			Geology ^e (%)			EC ^f (μS/cm)	
			AN	HS	LP	TG	CP	QF	PF	AS	L ^d	G	TWI	Qm		Tu
M1	0.20	3777 – 3900	85	13	2	85	15	0	14	0.9	1.9	9.6	100	0	0	35.7
M2	0.38	3770 – 3900	83	15	2	87	13	0	24	0.8	1.9	12.8	66	1	33	32.0
M3	0.38	3723 – 3850	80	16	3	78	18	4	19	1.0	2.0	9.4	59	41	0	62.4
M4	0.65	3715 – 3850	76	20	4	79	18	3	18	1.3	2.0	12.5	50	48	1	47.9
M5	1.40	3680 – 3900	78	20	2	78	17	0	20	2.5	1.9	11.8	70	1	30	37.0
M6	3.28	3676 – 3900	74	22	4	73	24	1	18	3.3	1.8	8.2	50	30	20	35.6
M7	1.22	3771 – 3830	37	59	4	35	65	0	12	0.4	1.7	10	87	0	13	15.3
M8	7.53	3505 – 3900	72	24	5	71	24	2	17	4.6	1.9	16.7	56	31	13	33.5

^a AN = Andosol; HS = Histosol; LP = Leptosol

^b TG = tussock grasses; CP = cushion plants; QF = *Polylepis forest*; PF = pine forest.

^c AS = average slope, L = flow path length ; G = flow path gradient; TWI = topographic wetness index (Beven and Kirkby, 1979).

^d L units in km.

^e Qm = Quimsacocha formation; Tu = Turi formation; Qd = Quaternary deposits.

^f EC = mean electrical conductivity. Data collected weekly for a three years period (June 2012-June2015)



Table 3. Main hydrometric variables of the catchments.

Catchment	Precipitation (mm yr ⁻¹)	Total runoff (mm yr ⁻¹)	Runoff Coefficient ^b	Average specific discharge (l s ⁻¹ km ⁻²)	Flow rates as frequency of non-exceedance (l s ⁻¹ km ⁻²)							
					Q _{min}	Q ₁₀	Q ₃₀	Q ₅₀	Q ₇₀	Q ₉₀	Q _{max}	
M1	1300	729	0.56	23.1	0.7	2.7	6.6	14.3	26.4	50.1	1039.0	
M2	1300	720	0.55	22.8	1.2	4.8	7.9	14.9	26.7	49.0	762.9	
M3	1293	841	0.65	26.7	2.3	7.3	10.8	17.7	28.1	52.4	894.2	
M4	1294	809	0.62	25.6	4.2	6.2	9.8	16.6	27.3	52.1	741.2	
M5	1267	766	0.6	24.3	1.5	4.1	8.3	15.3	26.9	50.8	905.7	
M6	1254	786	0.63	24.9	1.2	3.7	8.2	15.9	27.5	53.2	930.4	
M7	1231	684	0.56	21.7	0.3	1.8	5.2	11.0	23.3	53.9	732.0	
M8	1277	864	0.68	27.4	1.9	4.0	8.7	15.2	29.2	60.8	777.9	

^a Total runoff as a proportion of precipitation.



- 1 Table 4. Statistics of the $\delta^{18}\text{O}$ isotopic composition in precipitation and streamflow used as
- 2 input data for the MTT modeling.

Sampling Station	Altitude (m a.s.l.)	$\delta^{18}\text{O}$ (‰)				
		n ^a	Average	SE ^b	Max	Min
M1	3840	123	-10.6	0.06	-9.0	-12.6
M2	3840	124	-10.4	0.07	-8.8	-12.6
M3	3800	121	-10.7	0.05	-8.8	-12.1
M4	3800	122	-10.6	0.05	-8.7	-11.9
M5	3800	118	-10.5	0.06	-9.1	-12.8
M6	3780	121	-10.3	0.06	-8.9	-12.2
M7	3820	121	-8.9	0.15	-6.2	-13.9
M8	3700	118	-10.0	0.06	-8.3	-11.6
Upper Precip.	3779	137	-10.2	0.32	-1.2	-25.0
Middle Precip.	3700	134	-10.1	0.32	-2.7	-20.0

- 3 ^a n: number of samples collected.
- 4 ^b SE: Standard error.



1

Table 5. Statistical parameters of observed and modeled $\delta^{18}\text{O}$ for the stream at the outlet of the basin (M8)

Model	Observed $\delta^{18}\text{O}$		Simulated $\delta^{18}\text{O}$		Model Parameters ^b			MI ^c	(%)
	Mean (%)	σ^a (%)	Mean (%)	σ^a (%)	KGE ^a (-)	τ (days)	τ (days)		
EM			-10.02	0.52	0.63		191 (166 – 224)	2	
EPM			-10.02	0.52	0.63		109 (95 – 195)	4	
							η (-)	12	
							0.57 (0.52 – 0.96)		
DM			-9.95	0.64	0.5		664 (490 – 760)	11	
							τ (days)		
							Dp (-)	8	
							4.00 (2.80 – 3.93)		
GM	-10.05	0.45					392 (296 – 1478)	47	
							τ (days)		
							α (-)	9	
							0.70 (0.52 – 0.84)		
TPLR			-10.02	0.45	0.76		42 (18 – 93)	85	
							τ_f (days)		
							τ_s (days)	29	
							1623 (519 – 2638)		
							ϕ (-)	41	
							0.29 (0.14 – 0.51)		

^a σ = Standard deviation; KGE = Kling-Gupta Efficiency (Gupta et al., 2009). Statistical parameters of the simulated results correspond to the best-matching value of the objective function KGE.

^b τ = tracer's mean transit time; η = parameter that indicates the ratio between the contribution of piston and exponential flow; Dp = dispersion parameter; τ_f and τ_s = transit time of fast and slow flows in biweeks; ϕ = flow partition parameter between fast and slow flow reservoirs. (-) = Dimensionless parameter. Uncertainty bounds (5-95 percentiles) of simulated parameters shown in parenthesis were estimated using the generalized likelihood uncertainty estimation (GLUE, Beven and Binley, 1992).

^c MI = Measure of identification (Segura et al., 2012), i.e., ratio of behavioral parameter range to initial parameter range.



1

Table 6. Statistical parameters of observed and simulated $\delta^{18}\text{O}$ for all catchments using the exponential model (EM).

Catchment	Observed $\delta^{18}\text{O}$		Simulated $\delta^{18}\text{O}$			Simulated MTT ^b	
	Mean (%)	σ^a (%)	Mean (%)	σ^a (%)	KGE ^a (-)	(years)	(days)
M1	-10.63	0.37	-10.51	0.44	0.48	0.54 (0.48 – 0.63)	194 (171 – 227)
M2	-10.46	0.53	-10.51	0.63	0.61	0.43 (0.38 – 0.51)	156 (137 – 183)
M3	-10.64	0.23	-10.51	0.26	0.48	0.73 (0.64 – 0.86)	264 (232 – 310)
M4	-10.63	0.27	-10.51	0.3	0.48	0.67 (0.59 – 0.78)	240 (212 – 280)
M5	-10.51	0.39	-10.51	0.46	0.53	0.52 (0.46 – 0.61)	188 (165 – 219)
M6	-10.37	0.42	-10.43	0.5	0.59	0.52 (0.46 – 0.61)	188 (164 – 220)
M7	-8.93	2.92	-10.02	2.93	0.84	0.15 (0.12 – 0.18)	53 (45 – 64)
M8	-10.05	0.45	-10.02	0.52	0.63	0.53 (0.46 – 0.62)	191 (167 – 224)

^a σ = Standard deviation; KGE = Kling-Gupta Efficiency. Statistical parameters of the simulated results correspond to the best-matching value of the objective function KGE.

^b Uncertainty bounds (5-95 percentiles) of the simulated mean transit time (MTT) shown in parenthesis were estimated using the generalized likelihood uncertainty estimation (GLUE).

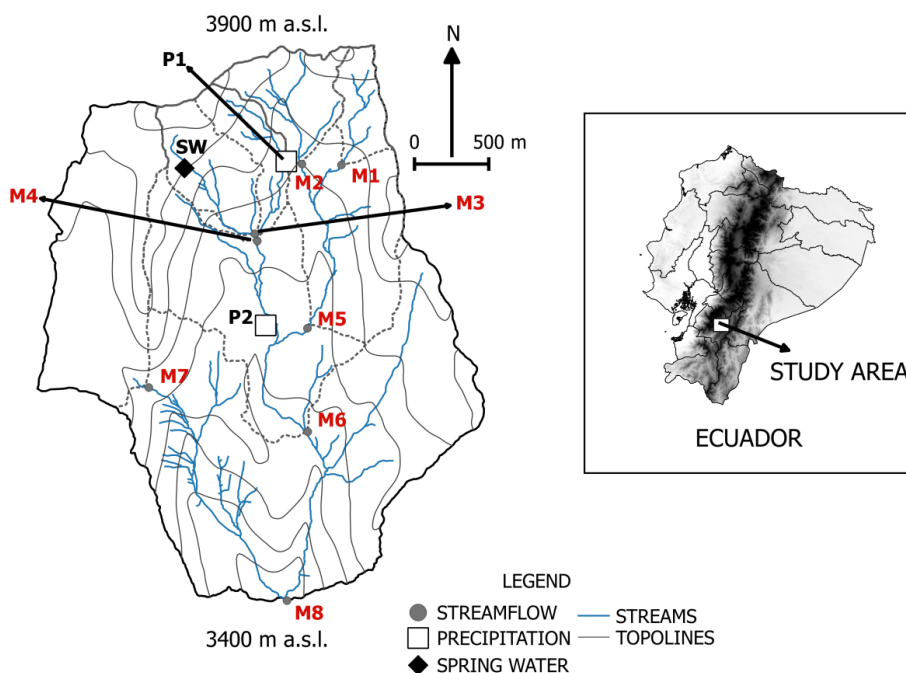


- 1 Table 7. Coefficient of determination (R^2) between the mean transit time (MTT) and i)
- 2 landscape features and ii) hydrological variables for each of the catchments. Catchments M3
- 3 and M4 (additional spring water source, see Figure 1) and M7 (at a flat hilltop disconnected
- 4 from the hillslopes) are not included in the regressions; except for electrical conductivity, i.e.,
- 5 all catchments are considered (Figure 9).

<i>Vegetation</i>		<i>General features</i>	
Cushion plant	0.29	Runoff coefficient	0.62
Tussock grass	-0.31	Total runoff	0.29
		Precipitation	-0.17
		Average specific discharge	0.21
<i>Soil Type</i>		<i>Streamflow rates</i>	
Histosol	0.13	Q ₉₉	0.42
Andosol	-0.13	Q ₉₀	0.18
		Q ₈₀	0.06
		Q ₇₀	0.09
		Q ₆₀	0.06
		Q ₅₀	0.01
		Q ₄₀	0.10
		Q ₃₀	-0.02
		Q ₂₀	-0.14
		Q ₁₀	-0.61
		Q ₅	-0.62
<i>Geologic formation</i>		<i>Water intrinsic properties</i>	
Quimsacocha	0.04	Electrical conductivity	0.90
Turi	0.12		
Quaternary deposits	-0.51		
<i>Topographic features</i>			
Average slope	-0.78		
Slope 0%–20%	0.85		
Slope 20%–40%	-0.90		
Area	0.13		
TWI	-0.03		
Flow path length (L)	0.23		
Flow path gradient (G)	-0.02		
L/G	0.23		

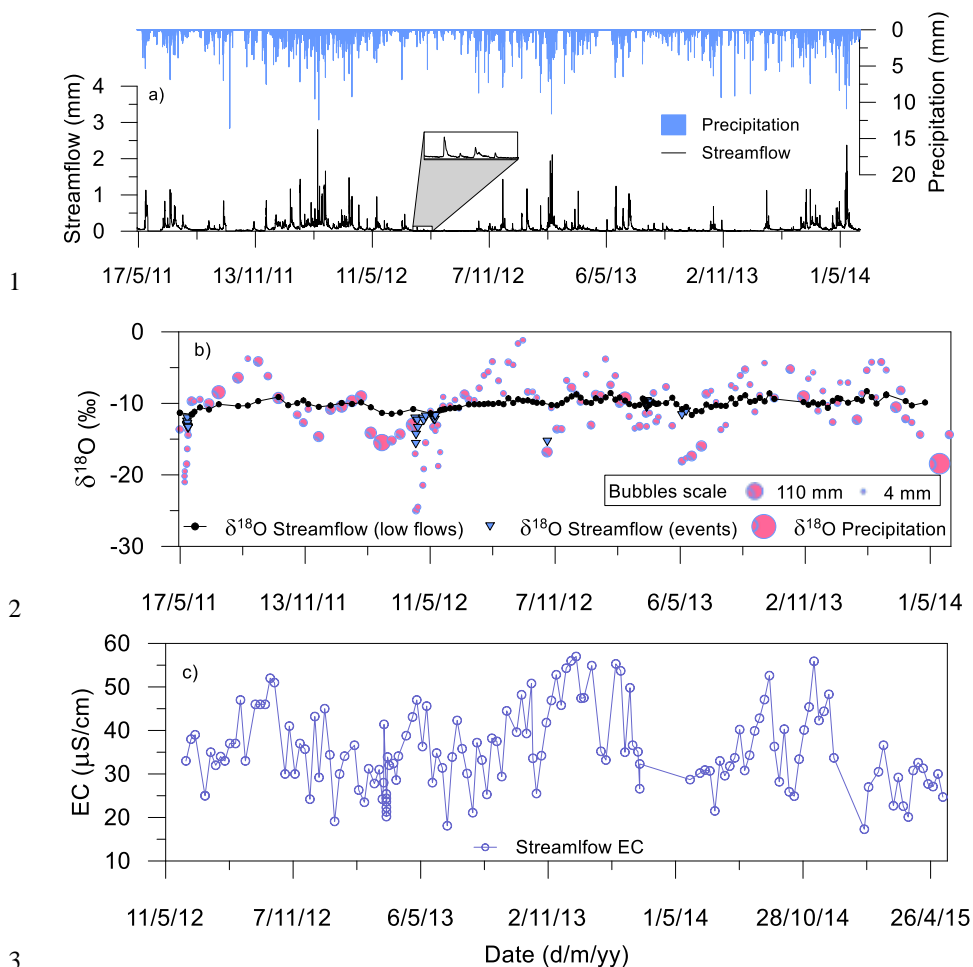
- 6 Signs indicate positive (no sign) or negative (–) correlation between parameters.
- 7 Values in bold are statistically significant to a 95% level of confidence ($p < 0.05$).
- 8 ^a TWI = Topographic wetness index (Beven and Kirby, 1979).

9



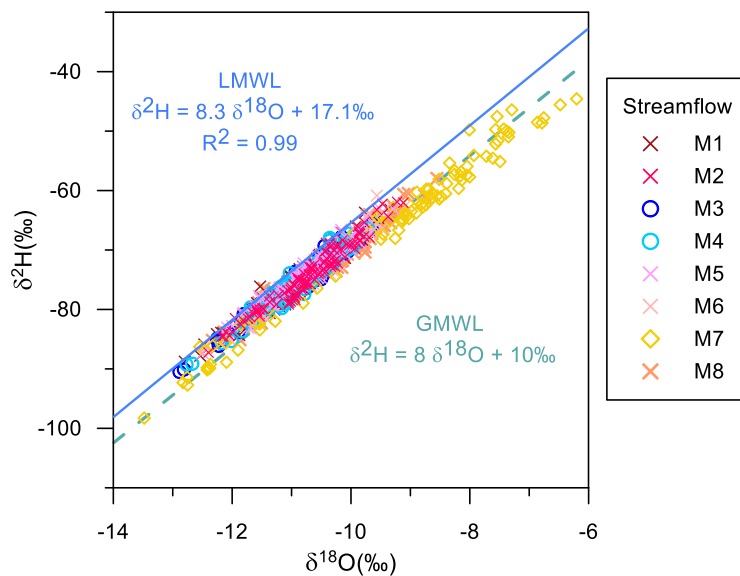
1
2
3
4
5
6

Figure 1. Location of the study area, and the isotopic monitoring stations in the Zhurucay observatory for: Streamflow (M), and Precipitation (P). SW is a spring water source upstream the outlet of catchments M3 and M4.



1
2
3
4
5
6
7
8
9
10

Figure 2. a) Hourly precipitation and unit area streamflow; b) $\delta^{18}\text{O}$ isotopic composition in precipitation and streamflow for 3 years (May 2011-May 2014); and c) electrical conductivity for 3 years (May 2012-May 2015) at the catchment outlet (M8, see location in Figure 2). The size of the bubbles in plot b) indicates the relative cumulative rainfall in millimeters for each collected sample.

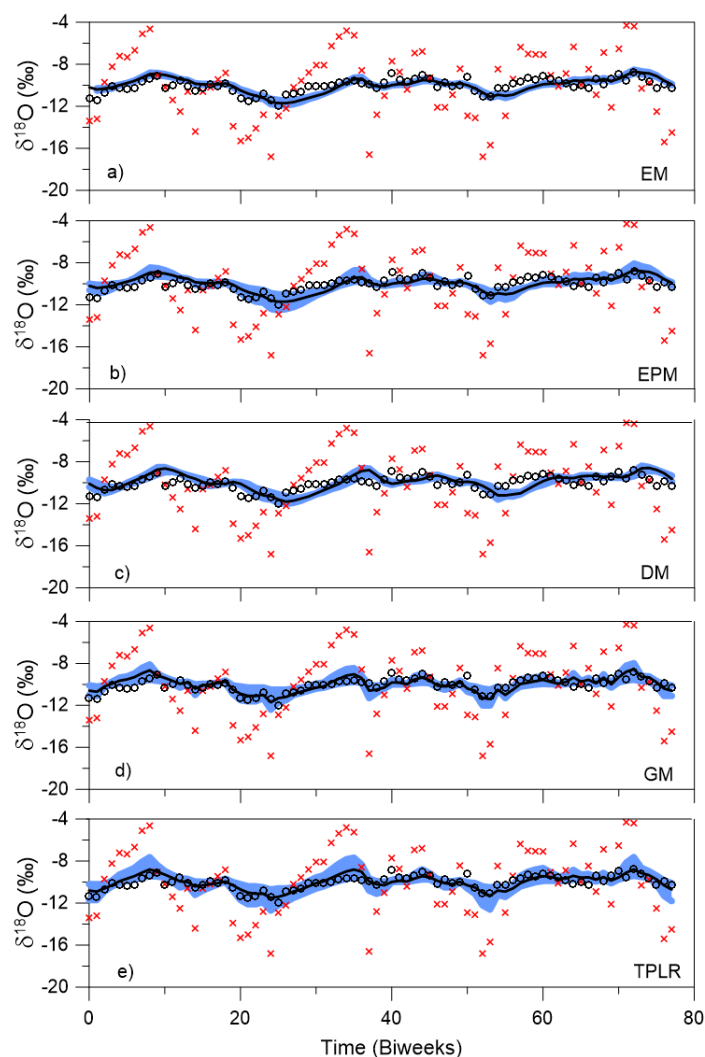


1

2

3 Figure 3. Relationship between the water stable isotopes ($\delta^2\text{H}$ and $\delta^{18}\text{O}$) in streamflow for
4 water samples collected within the Zhurucay observatory. The Local Meteoric Water Line
5 (LMWL) and the Global Meteoric Water Line (GMWL) are also plotted.

6



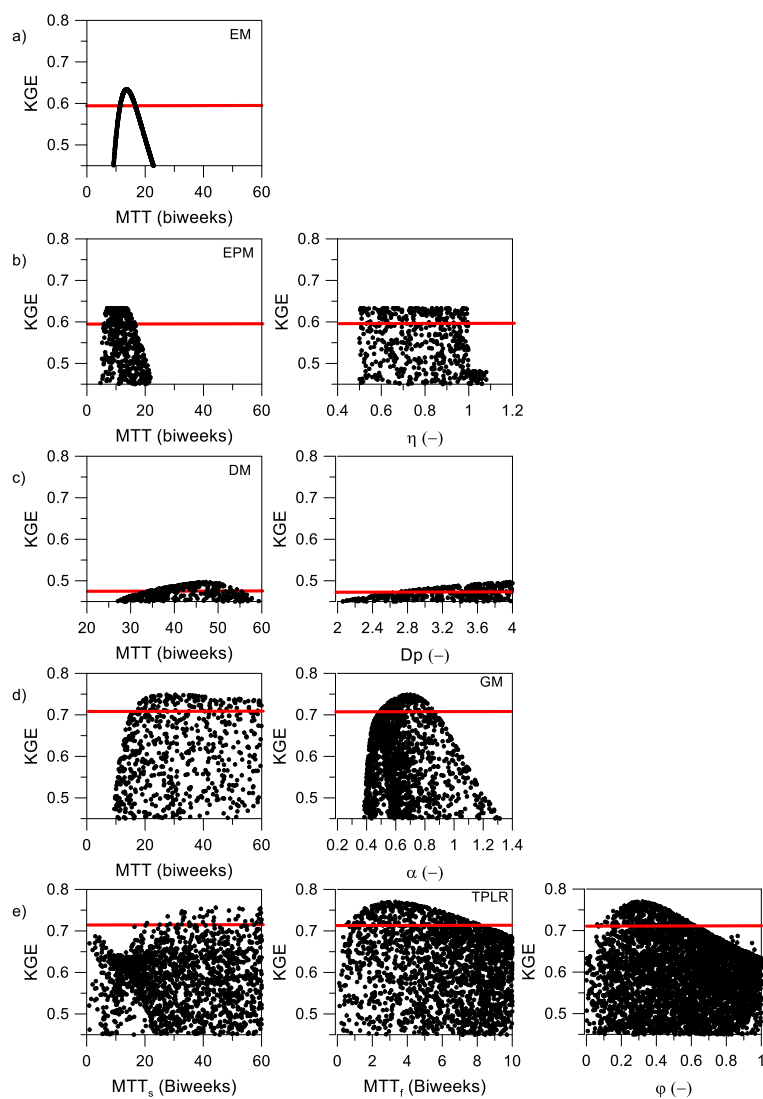
1

2

3 Figure 4. Fitted results of the five lumped parameter models used to simulate the temporal
4 variability in the $\delta^{18}\text{O}$ streamflow composition at the outlet of the basin (M8). (a) Exponential
5 model (EM); (b) exponential-piston model (EPM); (c) dispersion model (DM); (d) gamma
6 model (GM); and (e) two parallel linear reservoir model (TPLR). The open circles represent
7 the observed isotopic composition in streamflow; the red crosses represent the isotopic



1 composition in precipitation; the black line represents the best simulated isotopic composition
2 in streamflow according to the KGE (Gupta et al., 2009) objective function; and the blue
3 shaded area corresponds to the 5-95% confidence limits of the possible solutions from the
4 parameter sets within the range of behavioral solutions, i.e., solutions which yield at least
5 95% KGE.
6



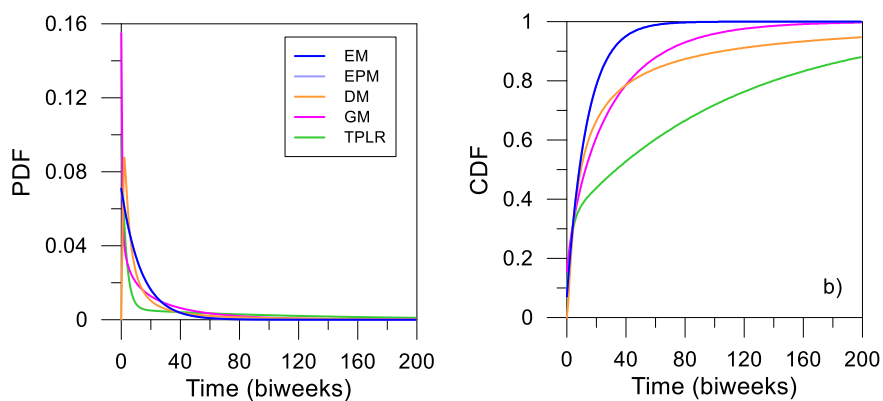
1

2

3 Figure 5. Monte Carlo simulation of the fitted parameters of the five lumped parameter
 4 models used to simulate the $\delta^{18}\text{O}$ streamflow composition at the outlet of the basin (M8)
 5 shown in figure 3. a) EM; b) EPM; c) DM; d) GM; and e) TPLR. The (-) symbol in the x-axes



- 1 denotes that fitting parameter is dimensionless. Horizontal red lines indicate threshold of
- 2 behavioral solutions (at least 0.95 of maximum KGE).
- 3

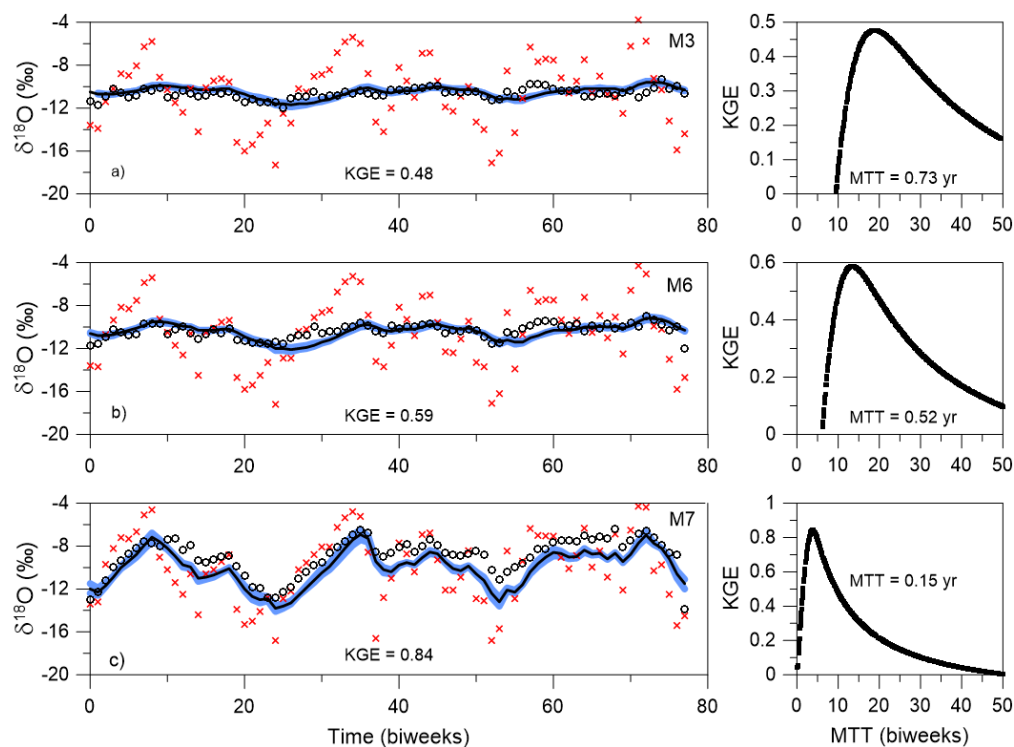


1

2

3 Figure 6. Probability (PDF) and cumulative (CDF) density functions for each transit time
4 distributions (TTD) used to simulate the $\delta^{18}\text{O}$ streamflow composition at the outlet of the
5 basin (M8). TTDs correspond to the best-matching values of the objective function KGE.

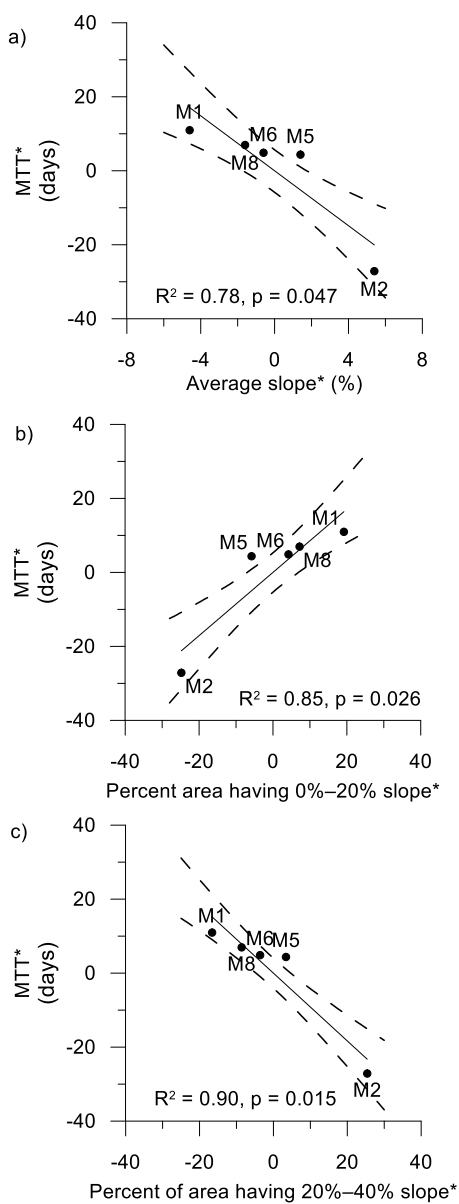
6



1

2

3 Figure 7. Fitted results and Monte Carlo simulations of the fitted parameters of the
4 exponential model (EM) used to simulate the $\delta^{18}\text{O}$ streamflow composition in the catchments:
5 a) M3; b) M6; and c) M7. The open circles represent the observed isotopic composition in
6 streamflow; the red crosses represent the isotopic composition in precipitation; the black line
7 represents the best simulated isotopic composition in streamflow according to the KGE
8 objective function; and the blue shaded area corresponds to the 5-95% confidence limits of
9 the possible solutions from the MTT fitting parameters within the range of behavioral
10 solutions, i.e., solutions which yield at least 95% KGE. Panels on the right represent the
11 explored parameter range for the MTT parameter and the KGEs associated to each of them.
12



1

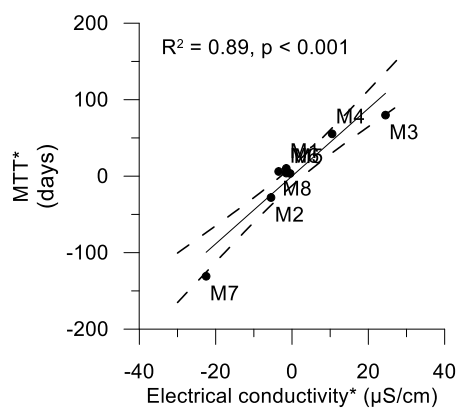
2

3 Figure 8. Correlations between mean transit time (MTT) and topographic indexes of the

4 catchments: a) average catchment slope; b) catchment area with slopes between 0% and 20%;



1 and c) catchment area with slopes between 20% and 40%. Catchments M3 and M4 (additional
2 spring water source, see Figure 1) and M7 (at a flat hilltop disconnected from the hillslopes)
3 are not included in the regressions. Solid lines are linear regressions and dashed lines are the
4 90% confidence intervals of the regressions. * Indicates parameters are normalized by their
5 mean
6



1

2

3 Figure 9. Correlation between mean transit time (MTT) and mean electrical conductivity for
4 weekly measurements of stream water samples collected during three years (June 2012-June
5 2015). Solid line is the linear regression and the dashed lines are the 90% confidence intervals
6 of the regression. * Indicates parameters are normalized by their mean.